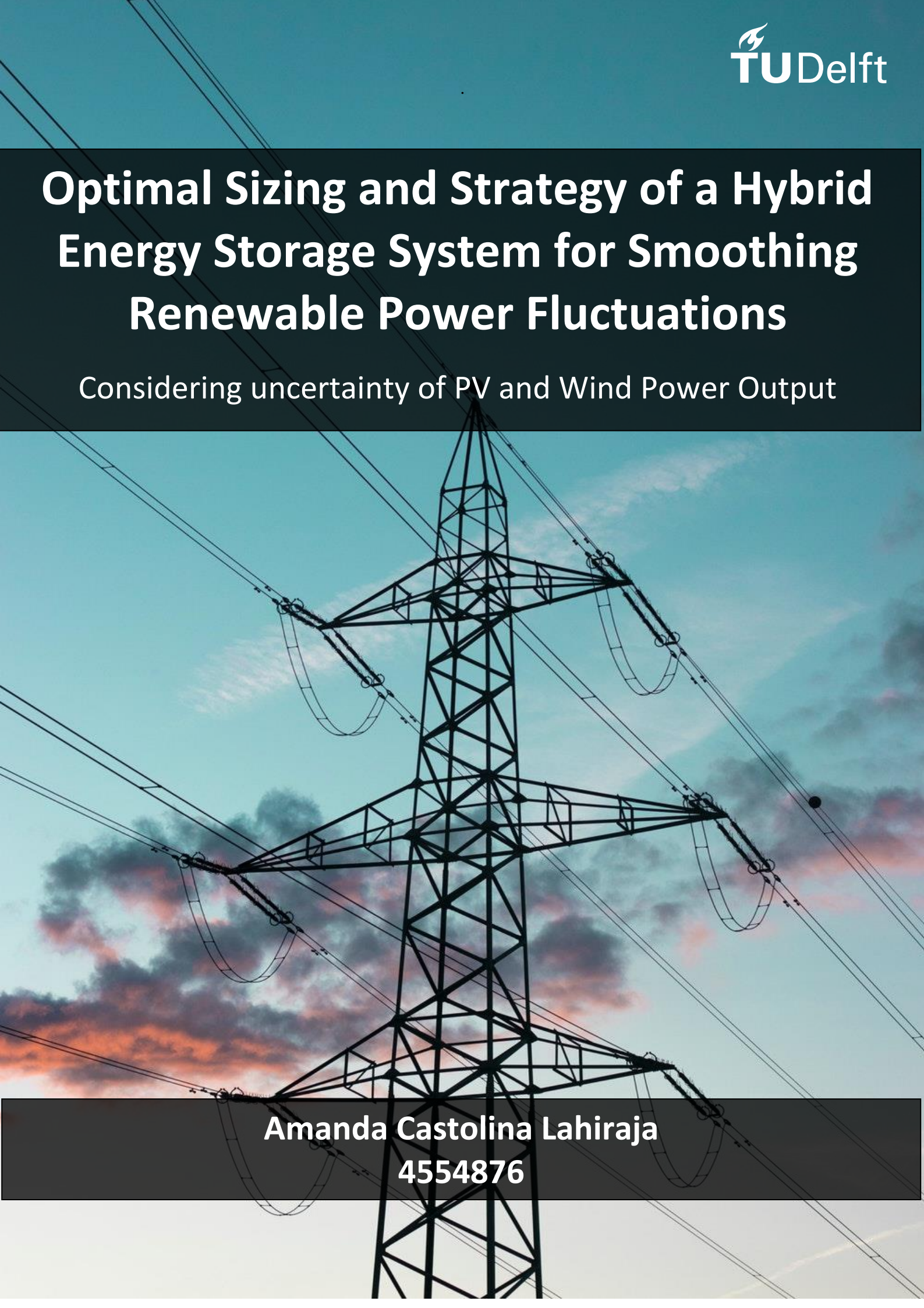# Optimal Sizing and Strategy of a Hybrid Energy Storage System for Smoothing Renewable Power Fluctuations

## Considering uncertainty of PV and Wind Power Output

Amanda Castolina Lahiraja
4554876

# Optimal Sizing and Strategy of a Hybrid Energy Storage System for Smoothing Renewable Power Fluctuations

## Considering uncertainty of PV and Wind Power Output

By

Amanda Castolina Lahiraja

in partial fulfilment of the requirements for the degree of

**Master of Science**
in Sustainable Energy Technology

at the Delft University of Technology,
to be defended publicly on Monday, August 26th 2019 at 13:00 PM.

| | | |
|---|---|---|
| Supervisor: | Dr. Milos Cvetkovic | TU Delft |
| Advisor | Aihui Fu | TU Delft |
| Thesis committee: | Dr. Milos Cvetkovic, | TU Delft |
| | Prof.dr. Peter Palensky, | TU Delft |
| | Dr.ir. Jose Rueda Torres, | TU Delft |
| | Dr. Zian Qin | TU Delft |

An electronic version of this thesis is available at http://repository.tudelft.nl/.

**TU**Delft

# Preface

*Alhamdulillahi rabbil alamin.* I owe everything I know today due to my personal experiences and the magical people I have aligned with, all because of God. From now on, I will always mention my guiders when celebrated for the version they helped me evolve into.

I would like to express my sincere gratitude to my supervisor, Dr. Milos Cvetkovic, who has guided me since day one of my internship until the final day of my thesis. I am really thankful for the kind attention and support he gave to make this an enjoyable journey. I would also say many thanks to my thesis committees, Dr.ir. Jose Rueda Torres, Dr. Zian Qin for the helpful feedback and comments. My sincere gratitude to Aihui Fu who has given me many insights through a lot of constructive discussions during the last nine months.

I am forever grateful to Indonesia Endowment Fund for Education that has provided my financial support for the two-year study in the Netherlands, and to UNDP for giving me the opportunity to help with the renewable energy project. It has been my dream to be able to give back some part of my knowledge that I have gained here to the community.

This journey will not be so fun without the presence of all my friends in Delft. Thank you for sharing all the laughter and joy with me, you guys are able to kept me sane during the most stressful moments of my uni life. My sincere gratitude to Denny Simanjuntak, whom have invested and believed in my dreams, simply because he saw a light in me that I'm only starting to discover recently.

Last but not least, if not due to the prayers from my families, I may not be able to reach the finish line. Thank you Papa Bob, Mama Rosta, Vino and Raka, for your endless support. For always believing in me and never giving up on me.

*This one is for you, Labuan Tiara Napitupulu. Indeed, "What is dead may never die."*

*Amanda Castolina Lahiraja*
*Delft, 22 August 2019*

# Abstract

Developing renewable energy sources entails new challenges which have not been faced previously by the traditional grid. One of the issues is the variability of renewable resources due to their characteristics of weather. The intermittent nature produces uncertainty in generation output, especially in solar and wind power generation. As penetration of both sources increase, variability will be more difficult to handle. And even as this issue is being resolved, another one, that of the application of an energy storage system has arisen. The energy storage is the current and typical means of smoothing wind- or solar-power generation fluctuations. Conducted research mostly developed an energy storage for only one technology, however, different technologies can be combined and complement each other which significantly improve the storage system's performance. In this research, a hybrid energy storage (HES) is proposed to mitigate power fluctuations of renewable plant output power.

This thesis aims to give understanding of the effective strategy of a hybrid energy storage for PV power output and wind power output fluctuation suppression. The strategy will stand as the foundation for a broader framework which aims to optimize the size of hybrid energy capacity to enable such application in uncertain condition. Wavelet power sharing method is proposed as the strategy to operate the hybrid energy storage using frequency-based method. The strategy can decompose the frequency component of renewable power quickly and allocate the power to the respective device. In this paper, battery and supercapacitor is adopted to meet the electric grid technical requirements for smoothing renewable power. The results show that the supercapacitor peak fluctuations of battery power are moderated by adding the supercapacitor, providing lower peaks and slower derivative of power fed to/drawn from the battery. The result from the power sharing is suitable in terms of improving the battery lifetime. Battery lasts for 1.3 years in a conventional energy storage system, while it can last up to 6 years in the hybrid energy storage.

After getting the optimal power allocation between storage devices, sizing the capacity of hybrid energy storage also considers uncertainty in power output. This research uses investment storage cost, penalty and life cycle cost as the objective function, while hybrid energy storage's state of charge and the power fluctuation performance as the constraint. The chance constrained programming is used to make the fluctuation of output power under a certain confidence level, which also meet the electrical quality and economy. The optimal solution of hybrid energy storage capacity is carried out by using genetic algorithm based on stochastic simulation. The results show that, with the confidence level of smoothing requirement up to 90%, system contains two energy storage has a lower total cost than a single-sourced energy storage.

# Contents

# List of Figures

# List of Tables

# 1

# Introduction

## 1.1. Renewable Energy Trends

Traditional ways of using fossil fuels to produce electricity have posed threat to the environment and population. Burning fossil fuels is the main reason that contributes to 13% increase in $CO_2$ emissions and the main cause of global warming, with 6°C increment of global average temperature [2]. Increased environmental awareness has made renewable energy an important topic of research and application nowadays. Throughout various parts of the world, high penetration of renewable energy sources (RESs) have led to increasing installed capacity and production levels for renewable electric generation.

Figure 1.1 shows that in electricity sector, renewable sources are forecasted to provide almost 30% of the world's power demand in 2023 [7]. Among all renewable sources, photovoltaics (PV) and wind turbines has a larger share of the generator mix in recent years. In 2023, solar PV and followed by wind is projected to meet more than 70% of total global electricity generation growth [8]. Current movements in support of renewable energy is pushing electric utility companies to develop more renewable forms of electricity generation as well as maintaining a specific percentage of renewale energy in the their mix electric generation portfolio.
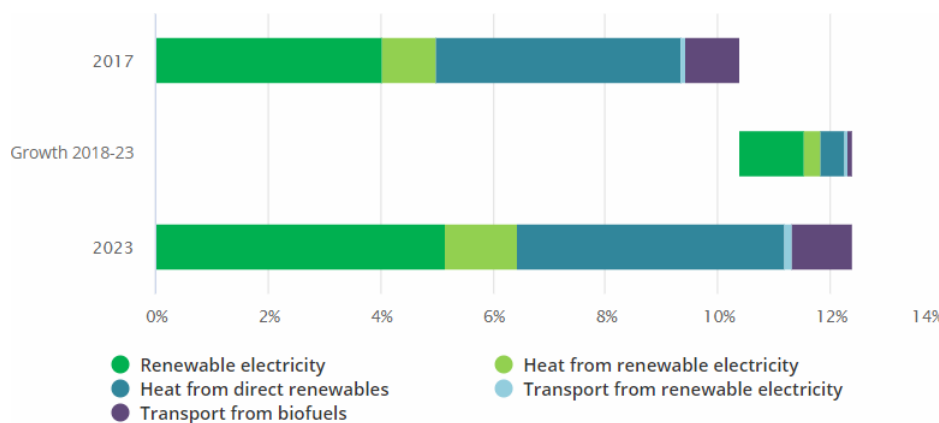


Figure 1.1: Share of renewable energy by sector in total energy consumption

According to Forecast International's Energy Portal, the market for renewable energy over the world is rising significantly also the main reason of the total growth of the world electricity consumption. Figure 1.2 shows the annual new installations of solar (PV) and wind energy installation actual data and forecast [1]. While some countries might experience some policy gaps to fully transition to commercial

market-based operation, wind turbines new installation is forecasted to be 75 GW in 2021. On the other hand, 2017 trend showed that new PV installations surpass the wind energy installations by almost two times larger. Until 2021, new PV installations are predicted to surpass 100 GW.
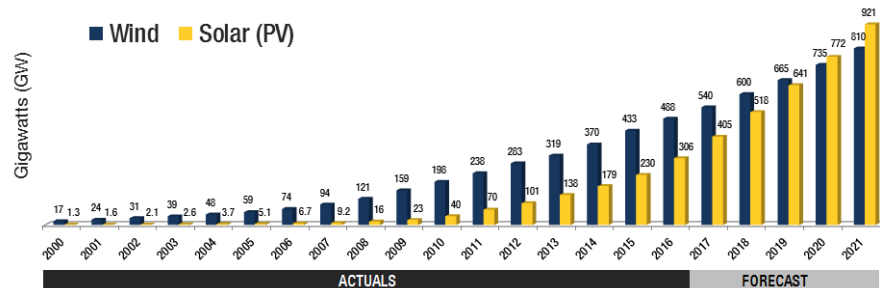


Figure 1.2: Share of Renewable Energy in Total Final Energy Consumption by sector [1]

## 1.2. 1000 Village Electrification Project

Access to electricity is critical for eradicating poverty and reducing inequalities. Being a developing country, Indonesia's electrification ratio is growing from 95.3% in 2017 into 98.3% in 2018. However, most of the provinces still have less electrification ratio compared to the average of the country. Nusa Tenggara, one of the eastern Indonesia's region, is still providing electricity for only 86.89% of the whole island's population.

Following the signing of Presidential Decree Number 59 year 2017 on Sustainable Development Goals (SDG), United Nations Development Programme (UNDP) Indonesia has established an official partnership with the local province's government to support the design and implementation of SDGs. Working alongside The Ministry of Energy and Mineral Resources, the non-governmental organization has commissioned three microgrid projects, providing power by combining PV systems, wind turbines and diesel power. In total, 1.2 MW of combined capacity of Photovoltaics (PV) as shown in Figure 1.3 and wind generation and a capacity of 144 kWh of diesel have been providing reliable energy for every hour of the day. With the green electrification of the villages, this action has allowed villagers to access their basic need, and also begin a phase of industrialization of the hybrid solutions.



Figure 1.3: Implemented Off-grid Project (copyright of UNDP Indonesia)

Following the successful implementation of isolated microgrid, UNDP is now choosing to connect the microgrid for traditional grid use. 1000 Village electrification project is one of the ongoing project that is being pursued. Currently, small-scale wind turbine and PV system are being built and feasibility study is being done on how the investment can be financially viable and technically feasible.

The Indonesian power system is vertically integrated, with Perusahaan Listrik Negara (PLN), which is Indonesia's state-owned utility company, owning the majority of generation as well as operating the transimission and distribution grid. From a technical perspective, the intermittent nature of PV systems and wind turbines' output power might lead to disturbing the continuous power to customers. An

additional grid code for Renewable Energy Generation Plants (REGP) is being introduced to renewable energy installations that are connected to the distribution grid with less than 10 MW of installed capacity. Renewable energy power plants owner need to comply with the local grid codes to ensure the standards comply with the requirement.

From an economic perspective, connecting renewable energy power output to the power grid also has some drawbacks. Total cost of the generated electricity is sold to PLN, therefore it is constrained by the fact that electricity selling price from independent power producer has to be less than the PLN's local generation cost. It is undesirable to have a high investment cost upfront and a low efficiency system, which is why the support of researchers along with the governments and electric utilities is the key to overcoming the aforementioned obstacles and improving the implementation of 1000 Village electrification project.

## 1.3. Integrating Renewable Electricity with Energy Storage on the Grid

Developing renewable energy sources entails new challenges which have not been faced previously by the traditional grid. One of the issues is the variability of renewable resources due to their characteristics of weather. The intermittency produces uncertainty in generation output, especially in solar and wind output power. As penetration of both sources increase, variability will be more difficult to handle. According to [9], almost 70% of solar capacity is affected due to passing clouds, while wind capacity highly varies on different seasons of the year. The renewable power production varies as the sun shines and wind blows, affecting the steady power supply to the consumer, as well as endangering grids operation in terms of different power quality issues, such as voltage variations and harmonics.

Power signal disturbances may cause stability problems in the current grid, both small and large disturbances. The conventional electric power systems may face many challenges, especially in on-grid areas, these issues are inevitable as the fluctuation in the output of renewable generation cannot be fully controlled and cannot be reliably predicted. The power output variations could affect daily operation of the system and the grid's management, including short-term variability (order of seconds to minutes) and long-term variability (order of hours), such as power interruptions, random component failures and accidents due to unpredictable weather conditions. The proper control and operation of such system will be very challenging because of the high uncertainty associated with RESs. In such cases, energy storage plays a vital role to stabilise such grids.

Energy storage most often has been associated with off-grid applications as backup power, enabling off-grid electrification systems. In the 21st century, grid-connected storage is a relatively new phenomena following the increasing installation of renewable energy production. As different issues entailed by the intermittency of solar and wind power production become clearer, a set of solutions are discussed to resolve them.

## 1.4. Thesis Project

### 1.4.1. Thesis Motivation

Prompted by the technical issues that have arisen due to the high penetration of intermittent RESs generators, deployment of energy storage in the power system is on the rise. Moreover, the decreasing trend in battery's price also accelerates the technology's implementation. Conducted research mostly developed optimal energy storage sizing for only one technology. However, experiments have been conducted on using energy storage to manage wind and solar uncertainty and can be roughly categorized into two types, a single source energy storage system and a hybrid energy storage system. In hybrid energy storage, different energy storage technologies so that they can operate together complementary and significantly improve the storage system's performance. In this research, hybrid energy

storage (HES) refers to more than one energy storage technologies with the coordinated operation to mitigate power fluctuations of wind and PV plant output.

Since optimal coordination between each technology in a HES may come up with economic considerations, this issue becomes an optimization problem. An effective strategy to obtain the optimal size of energy storage is necessary to cover before the implementation stage. In theory, a more substantial capacity of a storage system will produce smaller power fluctuation in the power grid. However, it entails a higher total cost, i.e. investment cost and operating cost. Moreover, the uncertainty of wind and solar power availability will force an even larger energy storage capacity to mitigate every possible power fluctuation in the future. Minimizing the total cost of the HES, while still delivering the intended service and maintaining the system's reliability becomes the priority from the renewable energy owner's perspective.

Most of the times, research authors assessed the sizing of HES and its operation strategy separately. However, an effective strategy between each technology in a HES will affect the optimal HES size ultimately. Therefore, it is necessary to understand both capacity sizing and the operation strategy to achieve a complementary performance in HES technologies.

### 1.4.2. Research Objectives

#### Main Research Goal

This thesis is aimed at understanding the effective strategy of a hybrid energy storage for PV power output and wind power output fluctuation suppression. The strategy will stand as the foundation for a broader framework which aims to optimize the size of hybrid energy capacity to enable such application in uncertain condition. The overall thesis objective is summarized in the following statement;

*Propose and implement a sizing methodology to determine the optimal size of hybrid energy storage for smoothing RESs energy generation.*

#### Research Questions

The main research goal is then translated into several research questions:

1. What is the effective strategy to operate a hybrid energy storage for smoothing application of intermittent RESs power output?

    (a) How does the power sharing between devices in a hybrid energy storage work?
    (b) To what extent the operation strategy will influence the energy storage lifetime?
    (c) How does the effective strategy affect the performance of the hybrid energy storage compare to a conventional storage system?

2. How to formulate the optimal hybrid energy storage sizing along with the power management system of the system considering uncertainty?

    (a) How is the hybrid energy storage characteristic modeled in the system?
    (b) What is the proposed optimization strategy's objective function?
    (c) Is hybrid energy storage a financially viable solution?

### 1.4.3. Thesis Outline

This thesis project aims to provide the readers the impact of using hybrid energy storage for a specific intention, which is to smooth the renewable power output fluctuation. The approach can be divided into two main focus. The first focus is how to operate the hybrid energy storage technologies and the

algorithm to share the effort between the components. The second focus is how to incorporate the uncertainty of renewable energy availability into the sizing of hybrid energy storage. Both approaches are organized in the following chapters, with the workflow illustrated in Figure 1.4.
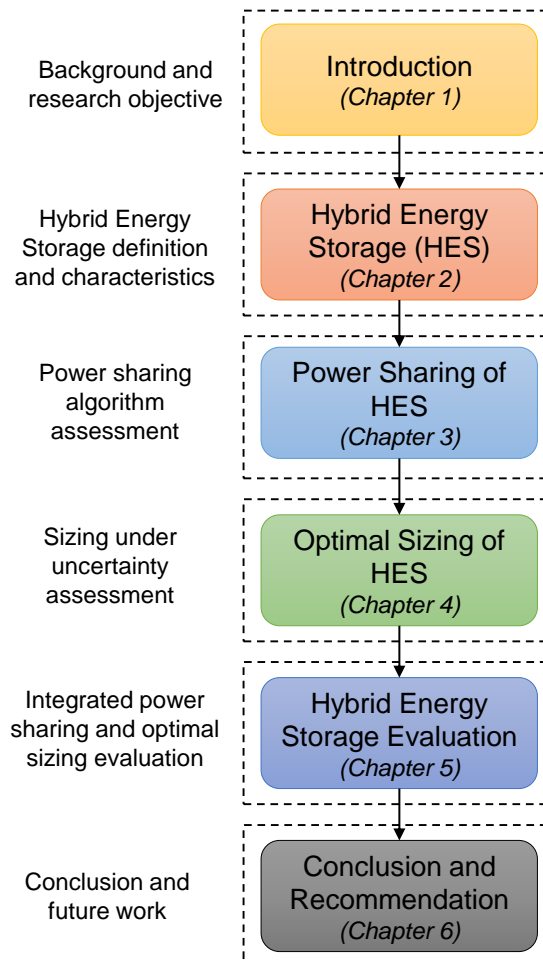


Figure 1.4: Research work flow

- Chapter 2: Hybrid Energy Storage

  This chapter describes the working principle of a hybrid energy storage system and its integration in an electric power grid in detail. Previous literature studies on hybrid energy storage's optimal sizing methodologies are discussed while the specific research gaps are identified.

- Chapter 3: Operation Strategy Formulation

  This chapter provides details of operation strategy to optimize power allocation among different energy storage technologies. The new control method based on wavelet power decomposition is proposed and then used for the formulation of an optimization problem.

- Chapter 4: Optimization Model Formulation

  This chapter describes the formulation of the optimization model in detail. Objective function and a set of constraints are formulated in equations form. In this research, a stochastic optimization is chosen to be the best approach to handle uncertain factors for the specified goal. A chance-constrained programming is incorporated with a genetic algorithm optimization to solve the hybrid energy storage sizing problem.

- Chapter 5: The Hybrid Energy Storage Evaluation For Smoothing PV and Wind Power Fluctuation

This chapter evaluates the proposed sizing methods on a system level. To evaluate the hybrid energy storage behavior, the wavelet-based power decomposition is conducted and compared with the initial system sizing methodology where the power sharing method is done in a conventional way. The performance and lifetime of energy storage device is conducted using a rain-flow cycle counting algorithm and compared with the conventional storage system.

- Chapter 6: Conclusions and Recommendations

    The last chapter provides answers for the research questions based on the simulation results. A set of recommendations for further improvement of this study is provided.

## 1.4.4. Research Contribution

Apart from the research goal, this research has contributions that can be used for other research in a broad application. More specifically, these contributions are:

1. This work provides a solution to an optimization problem that simultaneously takes into account capacity of an energy storage and its operation strategy. Most of the times, research authors assessed the sizing of HES and its operation strategy separately. However, in this research, the combined power allocating strategy and optimization algorithm are formulated, by also taking consideration of uncertainties and stochastic properties. It is necessary to understand both capacity sizing and the operation strategy to achieve a complementary performance in hybrid energy storage technologies.

2. This work provides a novel power allocation as a control strategy of a hybrid energy storage considering the device's technical requirements. A wavelet transform based energy/power management strategy for a hybrid battery/supercapacitor is proposed for a grid-connected power system to smooth PV and wind power output. Furthermore, this control strategy can potentially be used not only for a grid-connected power systems, but also off-grid systems or even electric vehicles application.

# 2

# Hybrid Energy Storage

In this chapter, at first the underlying hybrid energy storage concept is further explained. Section 2.1 explain the general overview of hybrid energy storage, the application and also the topology of the system. Section 2.2 elaborates the control and energy management concepts for hybrid energy storage. A comprehensive literature review on the hybrid energy storage capacity sizing is presented in Section 2.3, along with the state of the art of this thesis work.

## 2.1. Overview

As energy storage applications grow in complexity, Hybrid Energy Storage (HES) is becoming increasingly important to improve the power system's reliability with intermittent renewable energy. A typical HES consists of two storage devices which can complement each other [3]. There are two main complementary characteristics of an energy storage device, energy density and power density. The former represents the amount of energy that can be stored per unit volume or mass, while the latter can be denoted as the amount of power that can be delivered from a storage device with a given mass or volume. One energy technology device does not necessarily have a high energy density characteristics along with a high power density. Therefore, a HES mostly consists of technologies that can complement each other in these aspects.

Figure 2.1 shows the energy storage and power handling capacity of various storage technologies that are mostly used to store electrical energy. It can be seen that batteries and fuel cells have low power density, yet they have a high amount of energy that can be stored per unit mass. On the other hand, capacitors possess high power density characteristics, yet the technologies lack energy density.

An energy storage with low power density but high in energy density has a long period of life time even though regularly used. However, these devices usually have slower dynamic response [10]. On the other hand, a capacitor, even though in a much smaller size compared to the battery, is able to release energy quickly due to its high-power density characteristics. Each energy storage technology has a suitable application range. In a power system domain, energy storage with low power density but high in energy density like batteries are commonly intended for energy management. However, their slow response may create problems in the power control. On the other hand, high power density storage devices can deliver power in a fast manner, which can be the solution for fast dynamic response of a high power demand.

Although a number of technologies are mature and currently being developed, not one of the existing energy storage devices able to deliver high-power and high-energy capability in parallel. Therefore, a hybrid energy storage is needed to combine two or more energy storage technology devices to complement each other to achieve a reliable support for a power system. There are three important factors
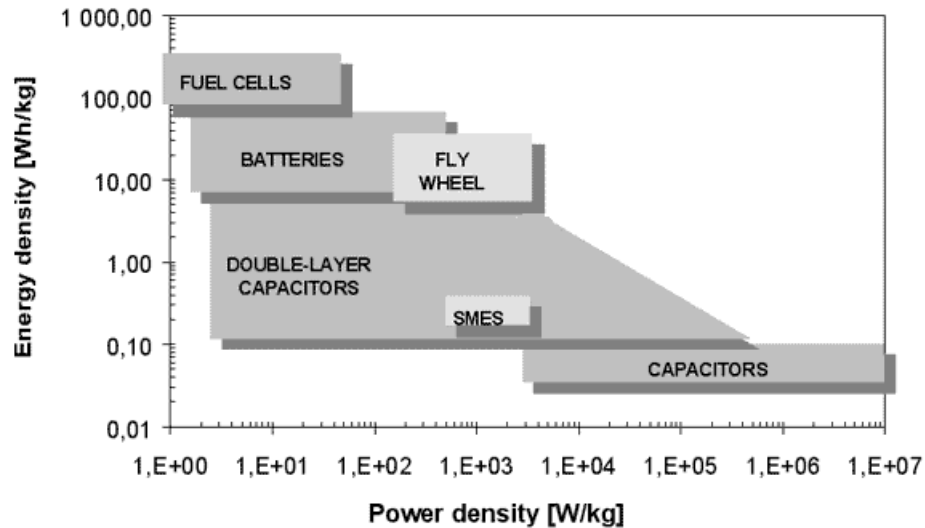
Figure 2.1: Storage Capacity and Power Handling Comparisons

to take into account in the design phase of implementing a hybrid energy storage in a power system [2]:

1. The technology choice of energy storage
   Over the wide range of parameters that storage technologies possess, the devices can be classified with respect to its function, consist of technologies that are intended for energy management and those that are designed for power quality.

2. The storage capacity and power
   The capacity of an energy storage is defined as the quantity of usable or available energy in the device, while power of the storage technology represents the device's maximum power output when operated in normal conditions.

3. Energy management of the HES system Ideally, the energy management of each energy storage technology and strategy as a whole system is the key to achieve a reliable system that can serve a specific application.

Figure 2.2 shows the example of combining an energy storage technology with its complementary device that have been used for various real-life applications. Generally two classes, near-term hybrids and long-term hybrids, can be distinguished. It can be seen that the supercapacitor/battery, fuel cell/battery, flywheel/battery, compressed air energy storage/battery, supercapacitor/fuel cell are commonly implemented in renewable energy storage application [2]. While the long-term energy storage hybridization are still under extensive research.

The most promising field that extensively uses hybrid energy storage in real life is the transportation sector, especially electric cars that are powered by fuel cells. In the automotive field, studies show that interfacing a supercapacitor with a battery can have a positive impact on the electric car's driving range. Some notable battery technologies used in conjunction with supercapacitor are lead-acid batteries, lithium ions and nickel metal hybrid batteries [11]. Supercapacitor energy storage is also complementary with a fuel cell technology to tackle the current fuel cell's slow dynamic response characteristics in the electric vehicles. Batteries and flywheels hybridization have also been coupled where the more power dense flywheel is responsible to the peak demand.

There are also hybrid energy storage applications on a household level, as well as regional level. Large scale wind turbines and PV systems are starting to implement hybrid energy storage to tackle the power forecast error impacts on the grid. The ability to store energy and inject the required power
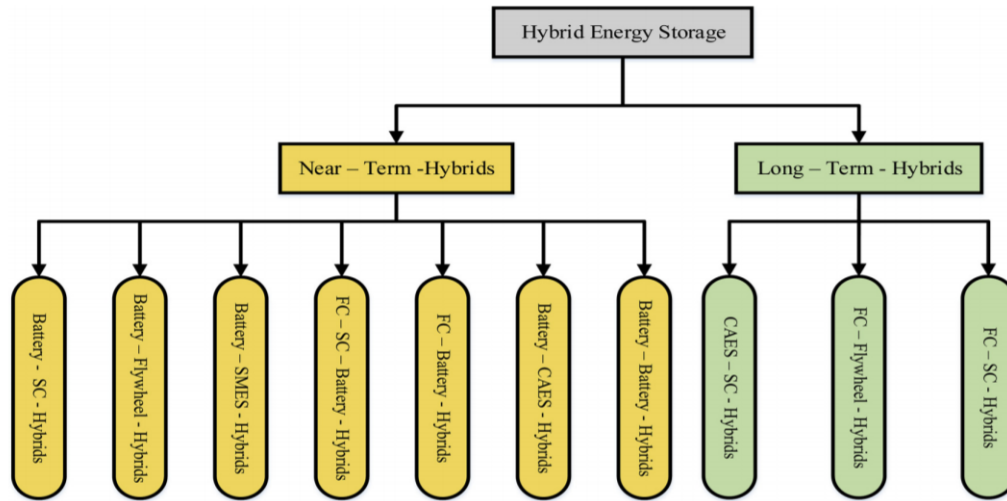
Figure 2.2: Various methods of storage hybridization combination [2]

to the grid has been addressed in [12] by using compressed air energy storage/battery as a real-life example from Figure 2.2. Ultimately, the possibilities of energy storage hybridization is countless, and each combination is able to serve its purpose if only correctly used with the right choices of storage devices, optimally sized, and operated with effective energy management.

## 2.2. HES Energy Management Approach

A single storage technology cannot always efficiently meet the requirements of highly variable charge and demand cycles, either in electric vehicles or renewable energy systems [4]. Such application does not necessarily follow a predictable charge and discharge profile, which entails non-stationary fluctuations in both power demand and supply. The non-stationary fluctuations may have different impacts on different energy storage technology. Therefore, optimizing allocation of power between each storage medium to achieve the desired effect remains a priority.

Figure 2.3 shows an overview of the basic concepts for HES that has been studied, mostly in the field of hybrid energy storage in electric cars. Generally, there are two classes that can be distinguished, rule-based and optimization-based energy management concepts. Both concepts are well suited for real-time applications with their own characteristics.
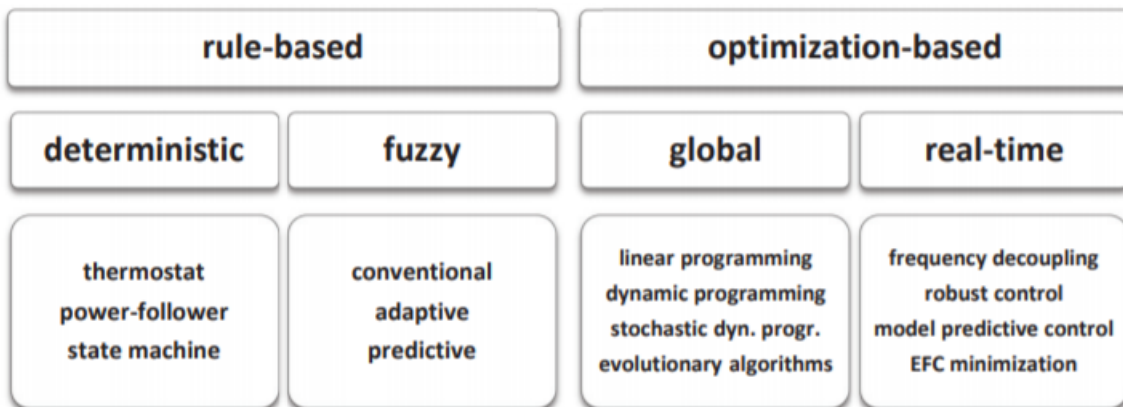


Figure 2.3: Control and energy management concepts for HES [3]

The simplest rule-based technology, thermostat concept, mainly uses a lower and upper State-

of-Charge (SOC) treshold to switch on and off between the "high energy" storage and "high power" storage. A more advanced concept, commonly known as fuzzy control, is used as a method to obtain a power split between both devices without switching, but with fuzzy-rules and its membership functions. Both deterministic and fuzzy control can easily achieve nearly optimal operation and handle measurement imprecision and component's variations.

On the other hand, the optimization-based technique offers a main feature which is the minimization of a cost function. An optimization-based energy management approach is the frequency decoupling, which can easily be applicable for real-time applications. Figure 2.4 shows the best visualization of typical frequency range and installed capacity of various energy storage devices. Pumped hydro and Compressed Air Energy Storage (CAES) are both the largest installations, with the lowest frequency range. On the other hand, supercapacitor device has the highest frequency range and the lowest installations.
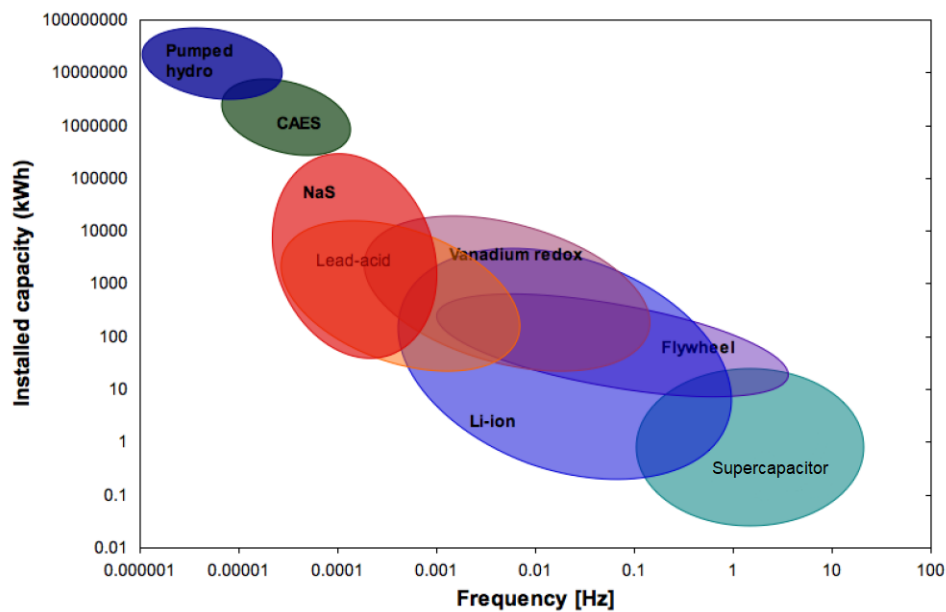


Figure 2.4: Typical frequency range and installed capacity of energy storage [4]

There are significant overlap between each storage device, hence the metric only offers partial insight of designing appropriate storage system. Ultimately, energy storage device selection requires both an analysis of frequency and capacity requirements of the power system. The variability of energy storage technology in a power system can be characterized by transforming the power signal into frequency domain [4]. In the frequency domain, fast changing and slow changing components of the power signal may each have unique storage technology requirements. The output from a wind turbine and a PV system may contain both high frequency bursts of electricity and more slowly varying fluctuations.

Conceptually, HES can be acknowledged as a filter bank, where fast-responding energy storage such as supercapacitor can carry high frequency supply and demand, while the burden of low-frequency components can be carried by batteries, pumped hydro or other large systems. Differentiating frequencies of power signal / electricity have been described for various storage systems by using filter-based methods. The frequency-based approach to design a hybrid energy storage has shown an improvement compared to single component storage systems. However, previous research primarily use a Fourier-based frequency analysis, which is not applicable for most real, non-stationary power systems [4].

## **2.3.** Capacity Sizing Methodologies

Figure 2.5 shows the mostly used sizing methodologies in finding the optimum capacity of a hybrid energy storage. One of the most important issue in HES implementation is to determine the optimum hybrid energy storage capacities. Over the years, many researchers have established methods or frameworks of optimal storage sizing. There is no clear superiority between one method over the other as authors usually do not reveal all technical details regarding their works, therefore it is rather difficult to explicitly state which sizing methodology is more efficient than the others.
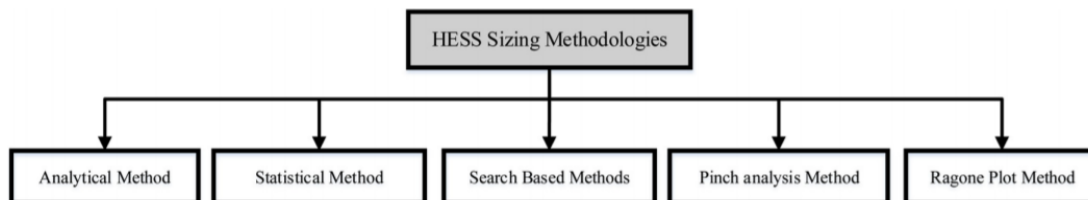


Figure 2.5: HES capacity sizing determining technologies [2]

1. Analytical Method
   As the most common used methodology, this method analyze a series of power systems configurations with the varying elements against the performance criteria. In general, the analytical methods that have been proposed consist of an objective function, constraints and solution methods. An advantage of this methodology is its independence of topology, technology and control strategy. The main disadvantage of this methodology is that it requires an all-knowing control strategy and only form the the problem to an energy balance.

2. Statistical Method
   Statistical method on the other hand gives more flexibility in a HES capacity sizing methodologies compared to the previous approach. An omniscient is not needed as the method does not necessarily need to determine numerous parameters. The method can obtain an accurate confidence level from a power generation variation histogram. For a short forecast application, statistical method is proven too be a powerful tool to size the storage capacity.

3. Search-based methods
   This method consists of mathematical optimization and heuristic methods. Some research have used the heuristic optimization methods because most often the objective function in sizing energy storage capacity has the characteristics of nonlinearity. Particle swarm optimization is proposed in [13] to obtain the HES capacity sizing to obtain the minimum cost. Genetic algorithm is used in [14] to determine battery and supercapacitor capacity that includes the 10-years battery replacement cost. Authors in [15] and [16] use discrete fourier transform to optimize the size of a HES, implementing a cost analysis which result in a linear objective function that is non-decreasing in the vector of storage sizes.

4. Pinch analysis method
   The method has does not extensively use long computational time, simple and flexible for determining the minimum energy points. This method is used with special emphasis on the efficient utilization of resources to determine the minimum renewable generator area, its extreme limits, and the corresponding storage capacity.

5. Ragone theory method
   Ragone plot as in Figure 2.1 is used to compare the performance characteristics of different energy storage. Sizing the hybrid energy devices can be achieved by using the Ragone plot as a constraint, which take the mutual restrictions between the rate capability and storage capacity of the energy storage under consideration. The ragone plot is used to determine the power density and energy density, by drawing a line and selecting the position of intersection between power demand and the energy storage capacity.

| Reference | Microgrid Configuration | | | Energy Source | Storage Technology | Sizing Method | Objective Function | Considered Factors | | | Summary & Advantages |
| --- | --- | --- | --- | --- | --- | --- | --- | --- | --- | --- | --- |
| | Type | Grid-connected | Islanded Mode | | | | | Installation cost | O&M | Lifetime | |
| Haihong Bian, et al. | AC | | ∨ | Wind | Battery, Supercapacitor | Ragone | Minimize investigation total cost | ∨ | ∨ | × | Sizing of storage in a wind/HESS system is studied considering the employed fuzzy-based control and State of Charge |
| P. Zhao, et al. | AC | ∨ | | Wind, hydro plant | HP & HE | AM | Wind power smoothing | | | | The storage capacity is obtained using a level below the net power curve |
| G. Wang, et al. | AC | ∨ | | PV | Battery, Supercapacitor | AM | Minimize investment cost | ∨ | ∨ | × | Unbalanced power is decomposed to four components using DFT, very short-term, short-term, intra-day and outer-day. Significant capital saving is the main advantage of this method. Under various operation modes, the minimum HESS capacity for a 30 MW PV power is found, considering the capital and O&M cost |
| S. Wen, et al. | AC/DC | | ∨ | PV, Diesel | Battery/Battery | SBM | Minimize investment cost | ∨ | × | × | Using FFT, unbalanced power is decomposed into various time-consuming components. Optimum HESS capacity with the cut-off frequency is obtained using PSO algorithm, showing that the cost is less than a single type battery |
| H. Jia, et al. | AC | | ∨ | PV, MT, FC, WT | Battery, Supercapacitor | SM | Extend battery lifetime | | | | A frequency cntrol method, using statistical model composed of time-domain simulaiton and statistical analysis is proposed. HES capacity at various probability levels are determined. Hysteretic loop to prevent over charge and discharge of the battery prolong its lifetime. The net power profile us used to size the capacity of HES |
| M. Masih-Tehrani, et al. | Hybrid Electric Vehicles | | | | Battery, Supercapacitor | SBM | Maximize battery lifetime | ∨ | × | ∨ | Genetic algorithm is used to find the optimum HES capacity. 10-years battery replacement cost is included and the result shows improvement of the battery lifetime and reduce the total HES cost over the 10-years |

Figure 2.6: HES smoothing schemes and sizing methods

| Reference | Microgrid Configuration | | | Energy Source | Storage Technology | Sizing Method | Objective Function | Considered Factors | | | Summary & Advantages |
|---|---|---|---|---|---|---|---|---|---|---|---|
| | Type | Grid-connected | Islanded Mode | | | | | Installation cost | O&M | Lifetime | |
| A.S. Jacob, et al. | AC/DC | | ✓ | | Battery, Supercapacitor, fuel cell | PAM | Minimize life cycle cost | | | | Pinch analysis method is implemented to size the production, load and energy storage's discharge curves. The curves describe a set of feasible capacities od the HES. The advantage of using this method is to analyse the demand and supply variability in different timescales (seconds to minutes, hours to days, and weeks to months) and selects appropriate storage options (short, medium, and long-term) |
| Y. Zhang, et al. | AC | ✓ | | Wind | Battery, supercapacitor | RPM | Minimize life cycle cost | ✓ | ✓ | ✓ | Mutual restrictions between the storage capacity and the rate capability is considered |
| D. B. W. Abeywardana, et al. | AC | ✓ | | PV | Battery, supercapacitor | AM | Minimize total cost | Only the capacity of supercapacitor is determined according to the net power profile | | | Supercapacitor energy controller is used for controlling the voltage and sizing the supercapacitor, which allows precise selection of the filter parameters and the supercapacitor's capacity |
| X. Feng, et al. | AC | ✓ | | Wind, PV | Battery, supercapacitor, flywheel, case | SBM | Minimize investment and operation cost | ✓ | ✓ | ✓ | Multi attribute combination optimization is conducted to obtain the HES capacity. Total annual cost, O&M and fluctuation smoothing ability are taken into account. This method offers an aggregate utility of each HES combination |
| S. Bae, et al. | DC | ✓ | | PV | Battery, SMES | AM | Maximize efficiency | Optimal efficiency points are selected for sizing th HES | | | The optimal efficiency points of the system are used to find the optimal HES capacity. The selected HES capacity can minimize the charging and discharging losses. |
| A. Maleki, et al. | DC | | ✓ | Wind, PV, Diesel | Battery, Fuel Cell | SBM | Minimize total annual cost | ✓ | ✓ | ✓ | The harmony search method determines the optimal capacity of the whole microgrid. Simulation results prove that battery energy storage is more cost-effective than using fuel cell storage system |

Figure 2.7: HES smoothing schemes and sizing methods (continued)

# 3

# Power Smoothing of Renewable Energy using HES

Section 3.1 explains the power fluctuation issue and the requirement of power injected into the grid. Section 3.2 explains the opportunity of using hybrid energy storage to mitigate the fluctuating output power, in conjunction with PV and wind power plants. Section 3.2 also explains the spectral analysis to obtain the target power that is capable of smoothing the fluctuation of the grid-connected generation system. Afterwards, an effective strategy, wavelet transform, is proposed in Section 3.3 as an appropriate tool in analyzing the transients in the power output. Later, the formulation of the method provides a means of assessing the optimal power and capacity of the Hybrid Energy Storage (HES).

## 3.1. Power Fluctuations of a Grid-Connected Hybrid PV-Wind Plant

This paper is focused on an AC microgrid with energy sources supported by hybrid energy storage. This section provides an overview of the hybrid system model of PV system, wind turbine and energy storage units, as well as power management method to keep the power balance inside the microgrid.

### 3.1.1. System Structures

The power generation system studied in this research, as illustrated in Figure 3.1, consists of a wind turbine system, a PV system, a HES, comprised of a battery and a super capacitor and a smoothing control. The combined rated power output of the wind farm ($P_w$) and PV system ($P_{PV}$)forms $P_{out}$. In order to solve the power fluctuation problem in $P_{out}$, a hybrid energy storage is employed to improve the power quality and achieve the allowable power ($P_{allow}$) at the point of common coupling (PCC).

The HES is responsible for the energy management between the output power from renewable energy sources and the allowable power at the PCC. At any time, the charging and discharging power of both battery and supercapacitor can be controlled to reduce the effect of $P_{out}$ power fluctuation and improve the power balance. It is assumed that the devices are installed closely and losses on the lines are neglected. $P_{allow}$ is the power injected into the utility grid, which can be calculated with 3.1.

$$P_{allow} = P_{out} + P_{HES} \tag{3.1}$$
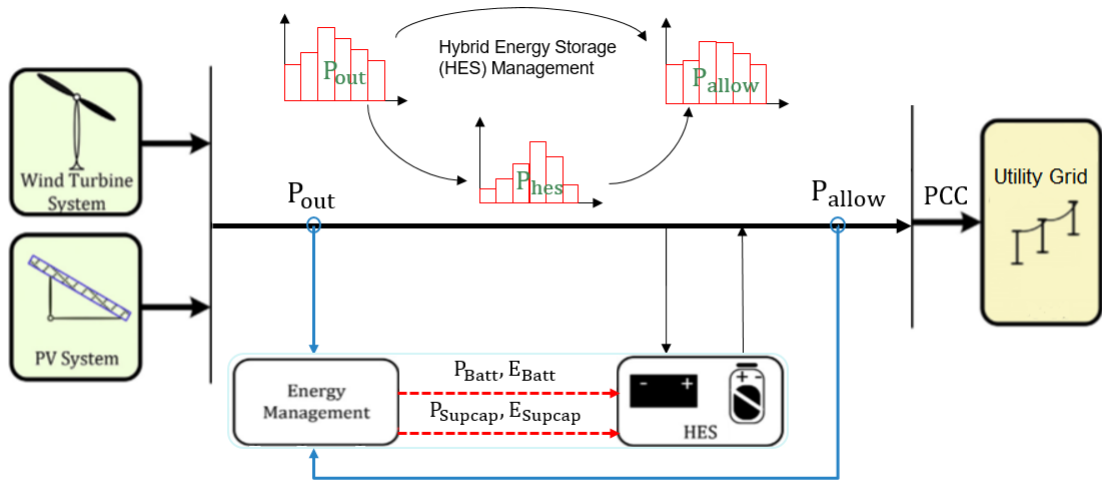
Figure 3.1: Outline of a wind and PV power generation system integrated with a HES

### 3.1.2. Renewable Power Output and Acceptable Power Fluctuations

This paper studies the maximum fluctuation of power injected into the grid according to the requirement adopted from the State Grid Corporation. The maximum power fluctuation of a renewable energy generation plant should not be more than 10%/minute of its installed capacity [17].

As shown in Figure 3.2, power fluctuation can be defined as the difference between the minimum and maximum power values measured at the the point of common coupling. At time t, $P_{Grid,before}(t)$ refers to the power value at the point of common coupling when correction action is not provided, while $P_{Grid,after}(t)$ refers to the value of power after correction action is provided. $\Delta P_{Grid,before}(t)$ and $\Delta P_{Grid,after}(t)$ are the power fluctuations of renewable energy generation before and after the suppression / smoothing control respectively. According to the historical data of $P_{Grid}$, $\Delta P_{Grid,before}(t)$ can be calculated by the following equation.
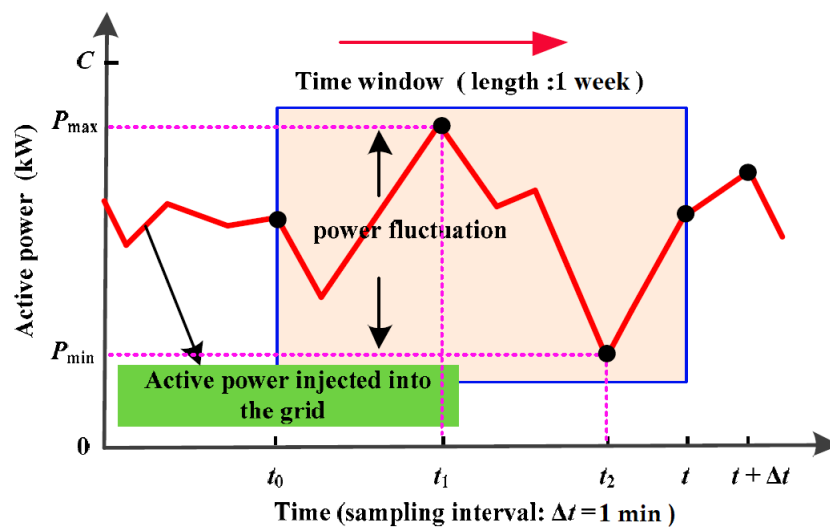


Figure 3.2: Renewable energy output power fluctuations

$$\Delta P_{Grid,before}(t) = P_{max,before}(t) - P_{min,before}(t), \text{i} \geq \text{j} \tag{3.2}$$

$$\Delta P_{Grid,before}(t) = P_{min,before}(t) - P_{max,before}(t), \text{i} < \text{j} \tag{3.3}$$

$$s.t. \begin{cases} [P_{max,before}(t), i] = f_{max}(\mathbf{A}) \\ [P_{min,before}(t), j] = f_{min}(\mathbf{A}) \\ \mathbf{A} = \{P_{\text{Grid}}(t_0), P_{\text{Grid}}(t_0 + \Delta t), ..., P_{\text{Grid}}(t - \Delta t), P_{\text{Grid before}}(t)\} \\ t_0 = t - 1sec \end{cases} \tag{3.4}$$

$P_{max,before}(t)$ and $P_{min,before}(t)$ refers to the maximum and minimum values of the set A respectively, where A is a set of power values measured at the point of common coupling before smoothing control provides the correction action. $\Delta t$, the sampling interval, is 1 minute and the time scale of the set $\mathbf{A}$ is 1 week.

In the same way, $P_{Grid,after}(t)$ can be calculated after the smoothing control is provided by the following equation.

$$\Delta P_{Grid,after}(t) = P_{max,after}(t) - P_{min,after}(t), \text{m} \geq \text{n} \tag{3.5}$$

$$\Delta P_{Grid,after}(t) = P_{min,after}(t) - P_{max,after}(t), \text{m} < \text{n} \tag{3.6}$$

$$s.t. \begin{cases} [P_{max,after}(t), m] = f_{max}(\mathbf{B}) \\ [P_{min,after}(t), n] = f_{min}(\mathbf{B}) \\ \mathbf{B} = \{P_{\text{Grid}}(t_0), P_{\text{Grid}}(t_0 + \Delta t), ..., P_{\text{Grid}}(t - \Delta t), P_{\text{Grid after}}(t)\} \\ t_0 = t - 1sec \end{cases} \tag{3.7}$$

where B is a set of power values measured after providing the correction action at the PCC, with the same time scale of the set A. The indices of the maximum and minimum values of the set B are m and n, while $P_{max,after}(t)$ and $P_{min,after}(t)$ refers to the maximum and the minimum values of the set B respectively.

According to the adopted requirement, power injected to the grid from renewable energy generation should not be more than 10 % of its capacity per minute, therefore, $\Delta P_{Grid,after}$ needs to meet the following constraint :

$$\left| \Delta P_{\text{Grid, after}}(t) \right| \leq P_{\text{limit}}, \forall t \in T \tag{3.8}$$

Where $P_{limit}$ refers to the maximum allowable power fluctuation of the wind and PV output power generation (10% of the installed capacity) and T = 00:00, $\Delta t$, 2 $\Delta t$, 3 $\Delta t$,..., 24:00 - $\Delta t$, 24:00 h.Based on the fluctuation constraints, it can be determined whether each successive time period meets the grid requirement. If the fluctuations from PV and wind power meet the requirement, there is no need to configure the energy storage system.

Figure 3.3 shows the algorithm procedures to obtain the grid acceptable power. The algorithm calculates the maximum range as shown in the blue box of power fluctuation that can be accepted by the power grid in the next second. The green line represents the original renewable energy output power fluctuation, while the red line represent the acceptable power value calculated by the algorithm. As shown in time interval 2, 3 and 5, the acceptable power will be automatically corrected as the maximum or minimum fluctuation value if it is beyond the range. On the other hand, the power value will remain the same as shown in time interval 1, 4, and 6.

According to the [18], the term of balancing power represents the excess or shortage capacity in the system, either in the form of excess available generation in PV and wind or shortage demand.
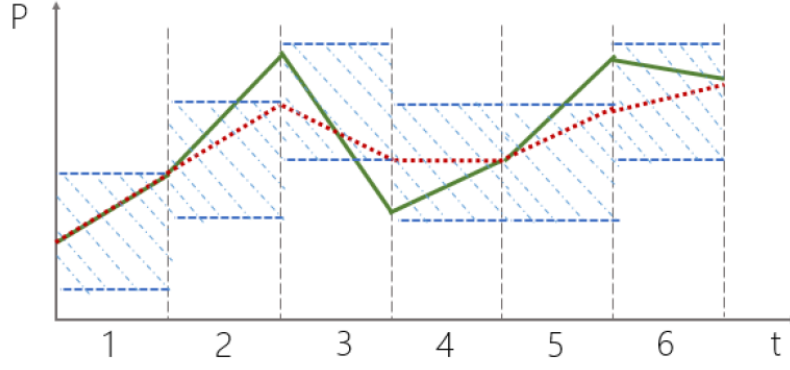
Figure 3.3: Grid Acceptable Power Algorithm

Balancing power will be the key factor of sizing the HES capacities. Based on Figure 3.1, $P_{out}$ is the sum of PV output power ($P_{PV}$) and wind output power ($P_w$). Hence, the difference between the value and grid acceptable power output value ($P_{allow}$) will form the balancing power ($P_{balancing}$). $P_{balancing}$ will make-up the difference between the smoothed power connected to the frid and the actual power from solar and wind hybrid system, and can be calculated according to Equation 3.9.

$$P_{balancing} = P_{out} - P_{allow} \qquad (3.9)$$

where:
$P_{balancing} > 0$ : Excess power generated by the renewable energy output needs to be absorbed by HES, therefore, HES is being charged.
$P_{balancing} < 0$ : Insufficient available power needed to be supplied by HES to match the grid acceptable power, hence HES is being discharged.

## 3.2. Power management strategy of a HES

The most common strategy to manage power between two different technologies in a hybrid energy storage is by supplying the demand power based on the high energy and high power specifications that each device possess. Frequently used approach is by commanding the high-power technology to supply the demand power up to its limits, then the high-energy technology will supply any demand power left which cannot be handled by the former device. This power distribution method is the conventional control strategy implemented in hybrid electric vehicles. Although, this simple power distribution strategy is able to command a hybrid energy storage to supply the demand power accordingly, a more sophisticated strategy will be broadly explained..

### 3.2.1. Choice of Storage Technology

To solve the power fluctuation problem in a grid-connected microgrid, choices of energy storage technology becomes necessary to ensure the improvement of the power quality. It needs to have a high degree of stability, as well as a good economical benefit, since it is intended to operate the system, i.e. charging and discharging the hybrid energy storage, in long-term.

As described in Section 2.2, the basis of the HES management strategy in this research is frequency-based management, which consists of splitting the overall balancing power into high- and low-frequency components. The balancing power's spectral decomposition has the advantage to divide the overall power fluctuations to different fast and slow components. Each component will then be tracked by a corresponding storage technology, based on the fact that each technology cycles energy within certain

frequency range. Depending on the time horizons, some energy storage technologies will be more advantageous, while other are less effective.

**Battery** is an essential part of the energy storage in a power system as it can store the energy produced by renewable energy power plants and provide electricity to the load or local grid simultaneously. The basic principle of a battery is converting chemical energy into electrical energy. There are two types of battery, primary battery which is non-rechargeable, and secondary battery which is rechargeable. In this research, a secondary battery technology called **lead acid battery** is used for several reasons. Firstly, lead acid battery offers a low investment cost, which is in favor to the off-grid or remote area storage system. Secondly, there are two types of lead acid batteries which have long been used for utility grid applications, i.e. sealed lead-acid and flooded lead-acid batteries. Generally, this technology has a downside such as its low number of cycles compared to lithium-ion batteries, the up-and-coming battery technology. However, from an economic perspective, sealed lead-acid battery is considered to be sufficient for smoothing power fluctuation and powering basic monitoring equipment.

**Supercapacitor** technology on the other hand, is a high-power energy storage device which can store electric energy using electrochemical double layers capacitor (EDLC). Renewable energy power plant's owner can use the high response speed of supercapacitor to react to fast changes caused by both PV and wind power fluctuation. Mainly used in transportation industry, new market opportunities such as smart grids and electrical power system, increases the opportunity for supercapacitor toa

Table 3.1 compares the battery and the supercapacitor performance. Compared to the batteries, supercapacitor possesses high power density and high charge/discharge rates. However, the technology has less energy density compared to lead acid battery. While batteries possess high energy density, they have low power density, giving low charge / discharge rates.

|  | Lead acid battery | Supercapacitor |
|---|---|---|
| Energy density | 10-100 Wh/kg | 1-10 Wh/kg |
| Power density | <1000 W/kg | <10000 W/kg |
| Charge time | 10 - 60 minutes | 1 - 10 seconds |
| Specific Power (W/kg) | 1000 to 3000 | Up to 10000 |
| Cycle life | 500 & higher | 1 million of 30000 h |
| Service life | 5 to 10 years | 10 to 15 years |

Table 3.1: Battery and supercapacitor performance comparison [5]

In electric vehicles application, supercapacitor is being strategically used to enhance the HES power and lifetime capabilities by buffering the battery and enabling greater braking and acceleration capabilities [19]. In a power grid system, there is a prominent benefit by using a hybrid energy storage to prolong the battery lifetime by reducing peak current stress on battery system. In effect, supercapacitor allows the battery to provide a mostly constant load profile with less rapid changes. Ultimately, compared with a battery-based energy storage system, a hybrid energy storage has a potential to reduce battery's charging cycles and improve its lifetime [11].

### 3.2.2. Energy Storage Lifetime Estimation

As is well-known, batteries are capable of ramping very rapidly, from zero power output to full capacity. Therefore, battery storage can respond to regulation signals with high performance. However, the frequent charge–discharge cycling of batteries when providing power fluctuation smoothing incurs a significant extra cost because it accelerates depreciation and shortens the life of the battery [20]. Thus, it is necessary to consider the battery life in this application.

In most types of battery technologies, their service life are highly influenced by their usage. The main factors which impact the battery's service life are temperature, calendar aging and cyclic aging [21]. In the long term, an increase in temperature causes higher electrochemical activity, thereby

diminishing battery capacity. Multiple research have shown a linear dependency between temperature and battery's cycle life [22]. On the other hand, calendar aging is affected by the corrosion process, which is independent of the battery's cycling behavior, while cycle lifetime is a number of complete charge and discharge cycles that a battery can undergo.

However, obtaining an accurate analysis of a battery's lifetime that and its degradation by taking into account all three factors will require extensive verification with laboratory experiments, which is not the focus of this research. To simplify the lifetime estimation model, only cyclic aging is considered. Moreover, the depth of discharge and the maximum state of charge are two manageable factors in the proposed control algorithms, which will mainly affect the life of battery. State of Charge (SOC), is the available capacity remaining in the battery, and its accuracy estimation is often important to provide precise parameters to improve battery lifetime [23]. Depth of Discharge (DOD), is an alternate method to indicate a battery's SOC, as the former increases, the latter decreases.

Figure 3.4 represents the number of cycles to failure at each depth of discharge for a lead acid battery. The cycle life versus DOD curve is acquired from the manufacturer's data and 10 data points are fitted in the curve. As shown in the figure, cycling the battery at a high DOD will dramatically reduce the number of charging-discharging cycles that the battery can undertake before it has to be replaced.
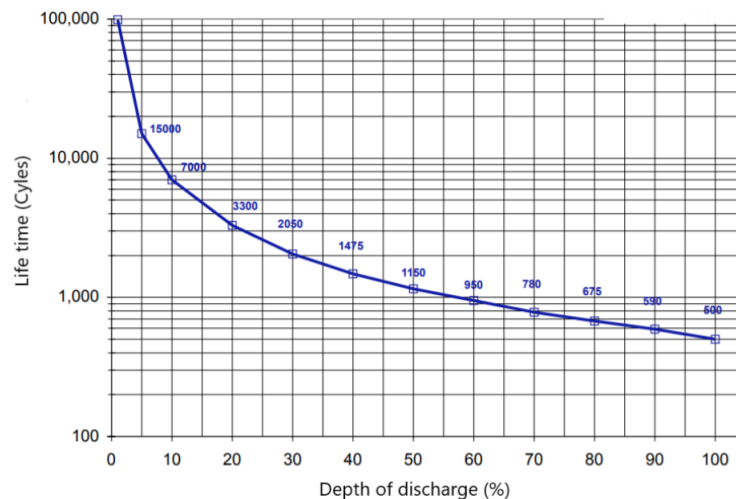


Figure 3.4: Lead acid battery's number of cycles to failure

It is worth to mention that the DOD and cycle life in Figure 3.4 represents DOD of complete cycles, by repeatedly discharging the battery and recharge it back to the full capacity. Otherwise, a cycle is considered as incomplete. Due to PV and wind power output variability, a grid-scale energy storage system is usually operated at irregular cycles, with more frequent charging/discharging process. In real operations, more incomplete cycles will happen and hardly run at regular cycles from 100% to a specific low DOD. Estimating a battery's lifetime while fully taking account of irregular operating conditions, such as partial SOC cycling and varying DOD is known as rather a difficult task. Therefore, building a degradation model that reflect irregular cycle impacts is necessary to obtain a battery's lifetime.

This research uses rain-flow cycle counting, which calculates the number of cycles at each DOD including irregular and regular cycles into the algorithm [12]. Commonly used in mechanical vibration applications, rain-flow cycle counting has been extensively used to identify an appropriate cycle counting method to estimate battery lifetime simply and completely [24]. Consequently, the lifetime of a battery can be calculated with Equation 3.10.

$$L_{\text{battery}} = \frac{T}{\sum_{i=1}^{m} \frac{N_t}{CF_i}} \tag{3.10}$$

Where T is the duration of simulation in years, $N_t$ is the number of cycles at each point of DOD. $CF_i$ is the number of cycles to failure at each DOD, and $m$ is the number of DOD ranges.

### 3.2.3. Frequency-based analysis of fluctuative power output

For wind and PV power generation, the fluctuation is widely distributed in various bands in the frequency domain [25]. The balancing power primarily contains two types of power fluctuations, smooth power fluctuation corresponding to a low frequency, and fast/frequent power fluctuations corresponding to a high frequency.

Since the HES includes both high and low speed responses, improved smoothing method can be obtained in comparison to single EES. The proposed power management is designed in such a way that the supercapacitor should be able to absorb the high-frequency power component of balancing power, leaving the steady component for the battery energy system. Recently, advances in the supercapacitor (SC) and battery's price reduction have made the SC and battery hybrid energy storage technically attractive. Principally, SC has high power density, high cycling life and high peak current handling capacities. However, compared to battery, SC has low energy density. On the other hand, battery is characterised by large energy density but low in power capacity. Therefore, the concept of the SC and battery hybrid energy storage is proposed in this research.

Power management of the hybrid energy storage is able to smooth the power output of the plant by reacting to the high variations in balancing power and to deal with these variations by operating in charging / discharging mode in order to keep the output power of the plant inside admissible values. The power fluctuation of different frequencies leads to various degrees of damage to the grid-connected power system. Therefore, it is necessary to first analyze the frequency characteristics of the balancing power, the amount of power to maintain the renewable energy output power and grid input power.

After obtaining the balancing power from Equation 3.9, the power signal can be broken down into the components spanning different frequency ranges, performing Fourier spectrum analysis method to convert power from time domain into frequency domain. A common method is by using Discrete Fourier Transform (DFT) analysis, as shown in Equation 3.11 until 3.16.

$$
\begin{aligned}
X(k) &= \text{DFT}(x(n)) = \sum_{n=0}^{N-1} x(n) W_N^{nk} \\
A(k) &= |X(k)| \\
f(k) &= \sum_{n=0}^{N-1} k \cdot f/N \\
k &= 0, 1, 2, \dots, N-1
\end{aligned}
\tag{3.11}
$$

Where N is the number of sampled data on a series of signals, $A(k)$ is the amplitude, $f(k)$ is the frequency, and $W_N = e^{j\frac{2\pi}{N}}$.

The result from decomposing the balancing power using DFT are

$$
\begin{aligned}
S_g &= \text{DFT}\left(P_g\right) = \left[S_g[1], \dots, S_g[n], \dots, S_g[N_s]\,\|\right]^T \\
f_g &= \left[f_g[1], \dots, f_g[n], \dots, f_g[N_s]\right]^T
\end{aligned}
\tag{3.12}
$$

Where DFT($P_g$) refers to decomposing balancing power signals using DFT and $S_g[n] = R_g[n] + I_g[n]i$ refers to the amplitude value at the frequency $f_g[n]$. The real part and the imaginary part of the amplitude are denoted by $R_g[n]$ and $I_g[n]i$ respectively.

$$f_g[n] = f_s[n-1]/N_s = (n-1)/(T_s \bullet N_s) \tag{3.13}$$

Where $f_s$ is the sampling frequency; $N_s$ being the number of sample points; and $T_s$ refers to the sampling interval, which is 1 second. According to the Nyquist principle, the spectrum can be symmetrically distributed around the frequency $f_N = f_s / 2$. In this research, the spectrum ranges from 0 to 0.5 Hz [=1/(1 s)]. Therefore, the spectrum of 0 ~ $f_N$ is representative of the whole sampled data.

$$\begin{aligned} D_g &= [D_g[1],...,D_g[j],...,D_g[\lfloor N_s/2\rfloor+1]]^T \\ f_{Ng} &= [f_g[1],...,f_g[j],...,f_g[\lfloor N_s/2\rfloor+1]]^T \end{aligned} \tag{3.14}$$

where $\lfloor N_s/2 \rfloor$ is the integral part of $N_s/2$ and $D_g[j]$ is the amplitude at the frequency $f_g[j]$. If $N_s$ is an odd number,

$$D_g[j] = \begin{cases} \sqrt{R_g^2[j]+I_g^2[j]}/N_s, & j=1,N_s/2+1 \\ 2\sqrt{R_g^2[j]+I_g^2[j]}/N_s, & j=2,...,N_s/2 \end{cases} \tag{3.15}$$

On the other hand, if $N_s$ is an even number,

$$D_g[j] = \begin{cases} \sqrt{R_g^2[j]+I_g^2[j]}/N_s, & j=1,N_s/2+1 \\ 2\sqrt{R_g^2[j]+I_g^2[j]}/N_s, & j=2,...,N_s/2 \end{cases} \tag{3.16}$$

According to [25], after obtaining the result from the Fourier-transform, power fluctuation can be decomposed into two sections based on varying frequencies:

1. Low frequency zone (0.01 Hz and below),

2. High frequency zone (0.01 Hz and above).

In [26], the above cutoff points are the dividing frequencies of the different HES devices, solely based on the response characteristic of each energy storage maximum response frequency. While the response time of a battery energy storage has been extensively discussed, cutoff points value are highly subjective. There is no obvious value that represent the cutoff frequencies for determining the energy storage capacities, which may vary based on the device in-house characteristics. In order to calculate the capacity of each energy storage as precise as possible, a more accurate energy sharing method is needed to make sure the designed HES is able to smooth out power fluctuations in all frequency bands.

## 3.3. Wavelet-transform-based power sharing

The main challenge of using HES is the power sharing between different technologies. For systems containing multiple energy storage systems, an appropriate power management is indispensable. Therefore, a power-sharing strategy of the HESS is developed to smooth the power fluctuations of PV and wind turbine.

### 3.3.1. Fundamentals of Wavelets

Wavelet transform is a signal processing method that has proven its usefulness in analysis of various types of signals. The tool is not a radically new method, as wavelet transform has recently been applied to variety of applications [5]. Typical ways of its utilization belong namely to, i) detection of signal discontinuities, ii) particular frequency detection, iii) signal suppression, iv) signal denoising and v) data compression.

Recently, wavelet transforms have been applied to analyze the power system transients, power quality, and fault detection problems [27]. One of the key properties of wavelet transform is its ability to locate short-time high-frequency features in a signal and at the same time resolve low-frequency behavior [28]. The method is knows to be a tool capable of representing non-stationary processes, which can extract characteristics of sharp and transient changes in a load profile [29].

A wavelet transform can be expressed in Equation 3.17.

$$W(\lambda, u) = \int s(t) \frac{1}{\sqrt{\lambda}} \psi \left( \frac{t-u}{\lambda} \right) dt \tag{3.17}$$

where $s(t)$ represents the input signal, $\lambda$ represents the scale parameter, and $u$ represents the parameter of the position. W can be denoted as wavelet coefficients, and $\psi$ is the mother wavelet which can be expressed in Equation 3.18.

$$\psi(t) = \begin{cases} 1 & 0 \leq t < \frac{1}{2} \\ -1 & \frac{1}{2} \leq t < 1 \\ 0 & \text{else} \end{cases} \tag{3.18}$$

The mother wavelet $\psi$ is a set of functions which can scale a sequence to a set of piecewise constant functions, and $\psi \left( \frac{t-u}{\lambda} \right)$, describes that the wavelet can be obtained by adjusting scale and position parameter to match any position of the original signal [29]. Therefore, the time-frequency analysis can be achieved.

Figure 3.5 shows a reference signal $x(n)$ being decomposed to different frequency ranges. Wavelet transformation of a signal contains the information regarding the low frequency content of the signal, which is called approximation coefficients (A) and the information regarding the high frequency content of the signal often, which is represented as detail coefficients (D).

$D_1$ refers to level 1 detail coefficient, which contains frequencies [f/2, f] of the reference signal x. If the input referense signal is being sampled at f, the detail signal can only contain f/2 Hz as its highest frequency, according to the Nyquist's theorem. The set of signals obtained eventually still represent the same original signal, but with different frequency bands. Afterwards, level k approximation coefficient $A_k$ can be further decomposed into more details and approximation coefficients, with the help of high pass filters and low pass filters, and down-sampling as calculated with Equation 3.19.

$$\begin{aligned} D_{k+1}[n] &= (A_k * h)[n] \downarrow 2 \\ A_{k+1}[n] &= (A_k * g)[n] \downarrow 2 \end{aligned} \tag{3.19}$$

The procedure is then repeated until the last approximated signal (A-n) has no longer transients or noise inside it. Therefore the number of decomposition levels will determine the accurate identification of the true components in the original signal and its noises. Naturally, more in-depth decomposition
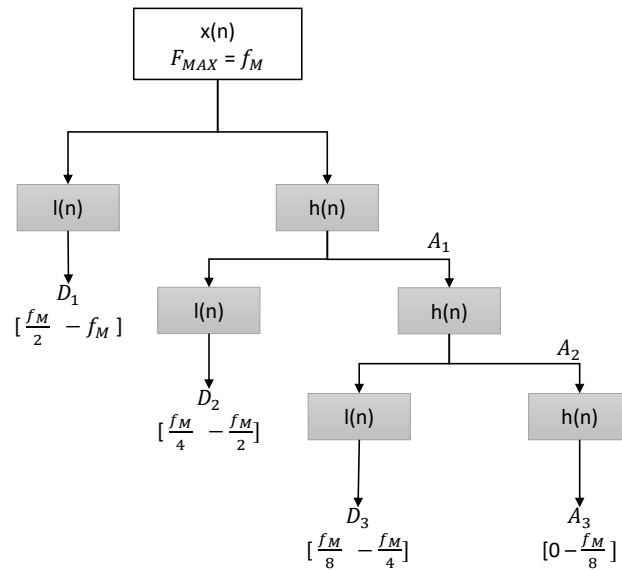
Figure 3.5: Wavelet analysis decomposition and reconstruction diagram

level will result in more accurate signal de-noising of the power spectrum. However, a great amount of decomposition layers must be considered properly to comply with computational effort in a realistic system. Presently, an established formula to obtain the maximum level of decomposition can be calculated with Equation 3.20 [30].

$$L = int[\log(N)] \tag{3.20}$$

where L is the number of decomposition level and N is the number of time series data.

### 3.3.2. Wavelet Transform Power Distribution Strategy

For illustration purpose, a three-level wavelet decomposition and reconstruction are used for signal decomposition and reconstruction process as shown in Figure 3.6. In this research, the balancing power obtained from Equation 3.9 is regarded as the original input signal. The application of wavelet analysis will determine the required capacity based on each electricity storage device.

↓ 2 represents subsampling by two, and the low pass and high pass filters are denoted as h and respectively. The approximation coefficient in the first and second level are the low frequency components derived from the balancing power signal. Similarly, the first and second level detail coefficient contains the high frequency component derived from the signal. The data size reduces by half in down-sampling operations while it doubles in up-sampling operations.

Eventually, the signal which contains only low-frequency components (A(n)) will be obtained, while the total high-frequency component signals will form the signal which only contains transients. According to the each device characteristics, high energy density of batteries can accommodate the low frequency content of the balancing power signal. On the other hand, the supercapacitors with high power density can be considered as peak balancing power buffer, which can accommodate the high frequency content part of the balancing power signal. The result of wavelet-based power sharing method is verified in Section 5.2.
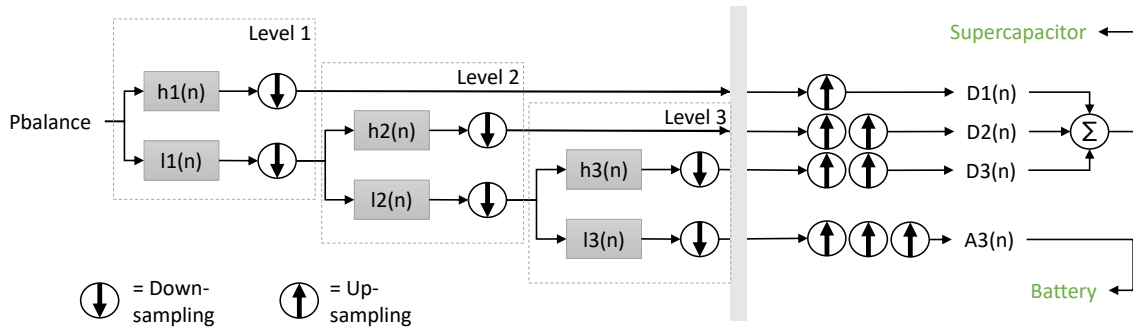
Figure 3.6: Three-level wavelet decomposition and reconstruction diagram

## 3.4. Conclusion

A hybrid energy storage power-sharing method has been developed and proposed in this research as a way to decrease wind farm and PV system power fluctuations. The method relies on the setting of one-second interval at a constant output level for the wind farm and PV system, using the storage system to absorb all deviations from the reference level at the point of common coupling. A power-sharing strategy on the HES is developed to smooth the power fluctuations of PV and wind turbine, in which power spikes are absorbed by supercapacitor energy storage, and battery energy storage only needs to provide low frequency part with less rapid transients.

# 4

# Hybrid Energy Storage Sizing Algorithm

*In the present paper, we focus on the optimization and the economic viability of storage from the point of view of the power producer who is evaluating the profitability of adding a hybrid energy storage system, which will be broadly explained in Section 4.1. On the one hand, if the grid does not have sufficient energy storage capacity, the fluctuating power generated by wind turbines or PV panels cannot be adequately stored. On the other hand, if the capacity is too large, the cost of investment will increase, which will be described in Section 4.2.*

## 4.1. Mathematical Model of HES

Based on the charge and discharge efficiency, the output power of the battery and supercapacitor can be calculated with the following equation.

$$P_{b,act}(t) = \frac{P_{\text{b,ab}}(t)}{\eta_{\text{d,b}}}, \quad P_{\text{b,ab}}(t) \geq 0 \quad (discharge) \tag{4.1}$$

$$P_{b,act}(t) = P_{\text{b,ab}}(t)\eta_{\text{c,b}}, \quad P_{\text{b,ab}}(t) < 0 \quad (charge) \tag{4.2}$$

$$P_{sc,act}(t) = \frac{P_{\text{sc,asc}}(t)}{\eta_{\text{d,sc}}}, \quad P_{\text{sc,ab}}(t) \geq 0 \quad (discharge) \tag{4.3}$$

$$P_{sc,act}(t) = P_{\text{sc,ab}}(t)\eta_{\text{c,sc}}, \quad P_{\text{sc,ab}}(t) < 0 \quad (charge) \tag{4.4}$$

Where $P_{b,ab}$ and $P_{sc,ab}$ is the absorbed power of the battery and supercapacitor respectively obtained after wavelet decomposition, while $\eta_d$ and $\eta_c$ are the discharge and charge coefficients for both battery ($\eta_{d,b}$ and $\eta_{c,b}$) and supercapacitor ($\eta_{d,sc}$ and $\eta_{c,sc}$). Incorporating charge and discharge efficiencies are necessary to look for consecutive charging and discharging cycles to obtain the size of each energy storage device.

After obtaining the actual compensation power $P_{b(t)}$ and $P_{sc(t)}$, the rated power of each energy

storage technology can be calculated by the following equation.

$$P_b = \max\left(\left|P_{b,\text{act}}(t)\right|\right) \tag{4.5}$$

$$P_{sc} = \max\left(\left|P_{sc,\text{act}}(t)\right|\right) \tag{4.6}$$

The power capacity of battery and supercapacitor is the maximum absolute value of the actual charging/discharging power. The accumulated energy for battery ($e_b$) and supercapacitor ($e_{sc}$ can be expressed by taking the integral of the rated power over period T.

$$E_b(t) = \int_0^T P_b(t)dt \tag{4.7}$$

$$E_{sc}(t) = \int_0^T P_{sc}(t)dt \tag{4.8}$$

Where T is the time period. Afterwards, considering the State-of-Charge (SOC) limits, the base capacity for battery ($E_{b,base}$) and supercapacitor ($E_{sc,base}$) can be calculated with the following equation.

$$E_{b,\text{base}} = \frac{\max\{E_b[t]\} - \min\{E_b[t]\}}{S_{u,b} - S_{l,b}} \tag{4.9}$$

$$E_{sc,\text{base}} = \frac{\max\{E_{sc}[t]\} - \min\{E_{sc}[t]\}}{S_{u,sc} - S_{l,sc}} \tag{4.10}$$

Knowing the amount of energy left in an energy storage device compared with the energy it had when it was full provides the user an indication of how much longer that device will continue to perform before it needs recharging. The State-of-Charge (SOC) of the HES can be calculated using the relationship between charging/discharging power in the energy storage equipment.

$$S_b = \frac{E_b^{ini} + \int_0^t \left(\eta_{c,b}P_{b,ab} - \frac{1}{\eta_{d,b}^x}P_{b,ab}\right)dt}{E_{b,base}} \tag{4.11}$$

$$S_{sc} = \frac{E_{sc}^{ini} + \int_0^t \left(\eta_{c,sc}P_{sc,ab} - \frac{1}{\eta_{d,sc}^x}P_{sc,ab}\right)dt}{E_{sc,base}} \tag{4.12}$$

Where $E_b^{ini}$ and $E_{sc}^{ini}$ are the battery and supercapacitor's initial capacity respectively.

The parameters of battery and supercapacitor are shown in Table 4.1.

|  | Lead acid battery | Supercapacitor |
|---|---|---|
| SOCmax | 0.8 | 0.95 |
| SOCmin | 0.2 | 0.05 |
| Charging efficiency (%) | 70 | 98 |
| Discharging efficienccy (%) | 80 | 98 |
| Rated power cost ($/kWh) | 488 | 366 |
| Rated capacity cost ($/kW) | 325 | 37000 |

Table 4.1: The parameters of Hybrid energy storage [6]

## 4.2. Objective Function

The main goal in this paper is to minimize the total cost of operating the renewable energy power plants with hybrid energy storage utilization. According to [31], there are two main approaches in the scope of energy storage cost analysis : total capital cost and life cycle cost. The former highlights the investment cost, which can cover the installation, purchase and delivery of an energy storage system. Most researchers express the total capital cost as a balance of power costs, which can be distinguished as per unit of power ($/kW) or per unit of energy ($/kWh). The latter consists of costs of operation and maintenance of an energy storage, as well as its recycling in addition to the total capital costs. From the perspective of the renewable energy power plants owner, life cycle cost parameter is more important because it comprises a more detailed calculation of the total energy storage's cost and considers its lifetime.

An essential financial indicator for the owner is the total spending on a technology delivered over the total life span of the project. By adding supercapacitor into the energy storage system, it is important to assess the economic feasibility and long run performance and comparing the benefits. Most research use conventional approaches that only taken into account the initial investment expenses, however, it does not reflect the true expenditure related to delivering the service.

Consequently, the initial capital cost and life cycle cost form the total cost of utilizing the hybrid energy storage system. The total cost is divided into three main elements, which are : capital cost, operation cost and replacement cost. The cost takes into account inflation and interest rate factors in the next 10 years of project lifetime. These discounting factors are assumed to affect all system elements uniformly, and applied to future expenditures to estimate the present value cost of the energy storage system.

Energy storage sizing optimization that gives the minimum total cost while meeting the power fluctuation requirement in the power grid application will establish the objective function. More in-depth explanation about the main elements of the total cost is described in Subsection 5.3.1 until Subsection 4.2.4.

### 4.2.1. Optimization objective

The optimization objective for HES capacity planning can be calculated by combining all three essential components of the total cost as shown in Equation 4.13.

$$minF_{cost} = F_{capital} + F_{operation} \tag{4.13}$$

Determining the appropriate size of the hybrid energy storage system component such that it has minimum capital, operating and replacement costs is the objective of the optimization problem in this research.

### 4.2.2. Capital Cost

Total capital cost is a one-time expenses incurred on the purchase of the whole energy storage components. In case of hybrid energy storage, the general capital expenses consist of unit capacity and unit power cost of the battery and supercapacitor, calculated according to 4.16.

$$F_{capital} = F_{BES} + F_{SC} \tag{4.14}$$
$$F_{BES} = C_{P,b}P_b + C_{E,b}E_b \tag{4.15}$$
$$F_{SC} = C_{P,sc}P_{sc} + C_{E,sc}E_{sc} \tag{4.16}$$

Where $C_P$ and $C_E$ are the cost of unit storage power and capacity respectively, applicable for both battery and supercapacitor with specific values as shown in Table 4.1. $P_b$ and $E_b$ are the rated value of optimal battery energy storage power and energy value obtained from 4.4 and 4.8. Both power and energy capacity are often used by researchers to indicate the size of an energy storage system because newer battery technologies have both properties de-coupled from each other [18]. Moreover, including energy and power capacity also indicate the minimal hours an energy storage is able to supply its rated power to a particular system.

### 4.2.3. Occurring / operation cost

The second essential element of the total cost refers to the operation expenses which take place on a regular basis. Primarily related with overall system management, this research consider a penalty cost which occur in a periodic fashion. This regular cost has to maintained due to imbalance in power fluctuation between renewable energy power plants and the allowable power of grid-tied. The penalty cost vary when the HES capacity changes and can be calculated by Equation 4.17 throughout the system lifetime.

$$F_{punish} = w_{cur} \sum_{t}^{T/\Delta t} P_{cur}(t) \tag{4.17}$$

where $w_{cur}$ is the unit cost of curtailment and $P_{cur}$ is the curtailed renewable energy, where:

$$P_{cur}(t) = | P_{allow}(t) - (P_{out}(t) + P_{HES}(t)) | \tag{4.18}$$

While operating all the system components, if the energy storage is not able to charge/discharge anymore, curtailment of the renewable power is considered to be feasible. The unused power from wind and PV systems therefore will be a waste, reducing the incentive of renewable energy investment over the project lifetime. Therefore, curtailment is expected to be at the minimu level, while wind and PV power output are desired to be utilized as much as possible.

The present value of operation cost that includes the penalty cost can be determined by using Equation 4.19 [32].

$$F_{operation} = \begin{cases} F_{punish} \left[\frac{1+f}{r-f}\right]\left[1 - \left(\frac{1+f}{1+r}\right)^n\right], & r \neq f \\ F_{punish} \times n, & r = f \end{cases} \tag{4.19}$$

where r being the annual real interest rate (%/year), f being the inflation rate of operation cost (%/year), and $n$ is the system life time in n years. Curtailment can be regarded as an inefficient use of renewable sources. In real-life application, a certain amount of energy curtailment is acceptable and most likely be unavoidable, especially when operating the hybrid energy storage with varying confidence level. However, it is necessary to avoid large-scale curtailment by minimizing it with hybrid energy storage, and ultimately achieve zero-curtailed energy in the power system.

### 4.2.4. Non-occurring / replacement cost

On the contrary with operation/regular cost, a replacement cost is a non-recurring costs which does not happen on a regular basis. Replacements take place when a certain component starts to deteriorate

and has to be replaced. The lifetime result obtained from Section 3.2.2 forms the replacement cost of the energy storage system. Replacement will take place when the battery reach the end of its lifetime within the life cycle of the whole system. By taking into account the inflation and interest rates, the present value replacement cost can be calculated by using Equation 4.20 [32].

$$F_{replace} = (C_{P,b}P_b + C_{E,b}E_b) \sum_{i=1}^{Nrep} \left[ \frac{1+f}{1+r} \right]^{\frac{N_i}{N_{rep}+1}}$$  (4.20)

where $N_{rep}$ is the amount of replacements within the life cycle of the system, and $N_i$ being the number of years. $C_{P,b}$ is the unit component cost of the battery energy system, while $P_b$ is the rated value of optimal power of the battery storage system. $C_{E,b}$ and $E_b$ are the cost unit of unit storage capacity and the energy capacity of the battery after the optimization. By calculating the lifetime of an energy storage using Equation 3.10, $N_{rep}$ is obtained simply by dividing the system life period in years with the life period of the intended technology.

It is worth to mention that replacement cost does not included in the objective function of the optimization problem. The life cycle cost is using the rainflow counting method, which considers the state-of-charge of battery in the hybrid energy storage as an input. The method then calculates the equivalent cycles and converted into an additional cost, adding more expenses to the objective function to identify the optimal capacity of the energy storage choice.

The proposed life cycle cost is assumed not to include the cost of either start-up or shut-down of the system, but can be associated as another single-payment capital cost. The purchasing of a new device is assumed to also include the cost of installing new energy storage devices and recycle cost of the older devices.

## 4.3. Constraints

The following constraints are necessary to be taken into consideration to ensure the optimization of the total cost of hybrid energy storage system.

In order to meet the requirements of the grid-connected, the fluctuations of the output power from wind turbines and PV system must be limited to a certain extent. In this paper, the power ramp rate (PRR) is used to evaluate the degree of power fluctuations on the power system. The PRR can be calculated by Equation 4.21.

$$R_{\text{prr},\Delta t} = \frac{P_{max,\Delta t} - P_{\min,\Delta t}}{P_{\text{n}}} \times 100\%$$  (4.21)

Where $R_{\text{prr},\Delta t}$ is the power ramp rate in time interval $\Delta t$. $P_n$ is the rated power of the wind turbine and PV system, $P_{max,\Delta t}$ and $P_{min,\Delta t}$ are the maximum and minimum power output of the microgrid respectively in time interval $\Delta t$. According to the requirements of the grid acceptable power in 3.1.2, the PPR limit can be defined as the maximum fluctuation for one minute. In the one minute interval, the PPR must be bounded in 4.22.

$$Max(R_{prr,1}) \leq 10\%$$  (4.22)

The real-time SOC is to be kept within the safe or desired range as the operation's security matter. In this research, it is expected that the real-time SOC of both battery and supercapacitor always fluctuate inside of the permitted interval, based on Equation 4.23 until 4.26.

$$S_{0,B} - \frac{\max\{e_b(t)\}}{E_{b,\text{base}}} \geq S_{L,B} \tag{4.23}$$

$$S_{0,B} - \frac{\min\{e_b(t)\}}{E_{b,\text{base}}} \leq S_{U,B} \tag{4.24}$$

$$S_{0,sc} - \frac{\max\{E_{sc}(t)\}}{E_{sc,\text{base}}} \geq S_{l,sc} \tag{4.25}$$

$$S_{0,sc} - \frac{\min\{E_{sc}(t)\}}{E_{sc,\text{base}}} \leq S_{u,sc} \tag{4.26}$$

where $S_U$ and $S_L$ are the upper and lower limits of SOC of the battery and supercapacitor.

$$\begin{aligned} P_{\text{pv}}(t) &\leq c_{\text{pv}} \quad \forall t \in T \\ P_{\text{w}}(t) &\leq c_{\text{w}} \quad \forall t \in T \end{aligned} \tag{4.27}$$

The PV and wind turbine maximum power outputs are constrained by 4.27 respectively.

## 4.4. Optimization Method Considering Uncertainty

The existence of many uncertain factors in renewable energy bring new challenges to the hybrid energy storage system planning. However, numerous methods that have been developed are based on accurate renewable energy output power profile without considering uncertainty. Sizing the energy storage for renewable energy applications with realistic representation of wind/solar power uncertainty remains a necessity.

### 4.4.1. Chance Constraint Programming

Sizing the energy storage in a power system with the utilization of renewable energy needs to have access to a realistic representation of wind and PV power uncertainty. A lot of developed models only used an accurate profile of wind and PV power, or a forecast system that still has errors from 10% up to 22% [14]. Given this problem, it is necessary to use a stochastic optimization method, that is suitable for solving problems that are associated with uncertain factors. A new method called chance-constrained programming is presented in this paper.

A Chance-Constrained Programming (CCP) can handle and model stochastic decision systems with assumption that the constraints will hold at least within a specified confidence level, provided as an appropriate safety margin by the decision-maker [33]. The constraint conditions are allowed to be dissatisfied within a risk level, so as to make the traditional rigid constraints keep a certain degree of flexibility while making a compromise between obtaining optimal objective and meeting the constraints. Thus, chance-constrained programming can be a useful tool to evaluate the probability or reliability of holding boundary constraints [34].

The general model for chance-constrained programming is shown in Equation 4.28 and 4.29.

$$\min f(x) \tag{4.28}$$

$$\text{s.t } \Pr\{g_j(x, \xi) \leq 0, j = 1, 2 \ldots n\} \geq \alpha \tag{4.29}$$

Where $\mathbf{x} \in \mathbf{R}^n$ is a vector of decision variables; $\xi$ is the stochastic vector; $f(\mathbf{x})$ is the objective function; $g_j(x, \xi)(j = 1, 2, ..., n)$ is the function's constraint; $P_r\{\cdot\}$ refers to the probability of the event $\{\cdot\}$ and $\alpha$ is the specified confidence level of the constraint function to be satisfied. In toher words, the constraints will be violated at most $(1- \alpha)$ of time.

Because of the uncertainties in renewable energy generation, mathematically the power fluctuation could be formulated as a stochastic optimization once. Chance constrained approach could be applied with an objective of minimizing the investment and find the most economical HES capacity, subject to the fluctuation constraint of wind and PV output power with the confidence exceeding required certain limits. The size will depend on a cost-risk analysis, comparing the cost of the HESS against the risk of violating the constraints, leading to a considerable reduction of the HES size.

The chance constraint-based HES cost optimization could be formulated by Equation 4.30 and 4.31.

$$minF_{cost} \tag{4.30}$$
$$\Pr\{|\Delta P_t| - 10\% \text{ of Total Capacity } \leq 0\} \geq \alpha \tag{4.31}$$

In this research, the limited power ramp rate from Equation 4.21 is translated into the confidence level value as stated in Equation 4.31. $\Delta P_t$ is the difference of $P_{max,\Delta t}$ and $P_{min,\Delta t}$, the maximum and minimum power output of the microgrid respectively, in time interval $\Delta t$. According to the requirements of the grid acceptable power, the 10% of the total renewable plants capacity limit can be defined as the maximum fluctuation. It should be stated that highly violating the power fluctuation grid code may result in unsought and possible extreme financial penalties. Therefore, the constraint could be violated under some exceptional cases, but the probability of such power fluctuation violation must be less than a specified rate.

While CCP has been proved to be a powerful tool to consider the uncertainty in model parameters, the realization of the method has been limited by the strict mathematical structures required by conventional procedures such as linear and linear programming [35]. The application has to consider an optimization solution that can offer flexibility in CCP problem formulation.

### 4.4.2. Genetic Algorithm

Genetic Algorithm (GA) is an optimization tool for a stochastic problem. Using a population based tool, the algorithm initially set a randomly generated population to set the initial solutions to the multi-objective problems. This fitness of the solution, or "fitness function", is used to evaluate each solution individually an rank them according to their fitness value. The optimal solution is obtained by going through different operations such as crossover, reproduction and mutation.

Figure 4.1 represent the Monte Carlo simulation embedded with genetic-algorithm approach is employed to solve optimization problem as described in Equation 4.13. Dealing with a system with an integration of PV and wind power output, uncertainty brings new challenges which deterministic techniques are unable to handle. Therefore, GA technique can bring flexibility to handle a stochastic problem with a chance-constrained optimization.

In this research, numerical models such as Monte Carlo (MC) simulation is incorporated into the GA search process. The general idea of using the MC simulations is to check whether the solution meet the chance-constraint in the GA fitness function. If the chance constraint is not met, a certain penalty is exacted, reducing the fitness of a certain strategy. The best solution is evaluated based on both the objective function and the ability to meet the constraint for a specified chance of MC realizations.
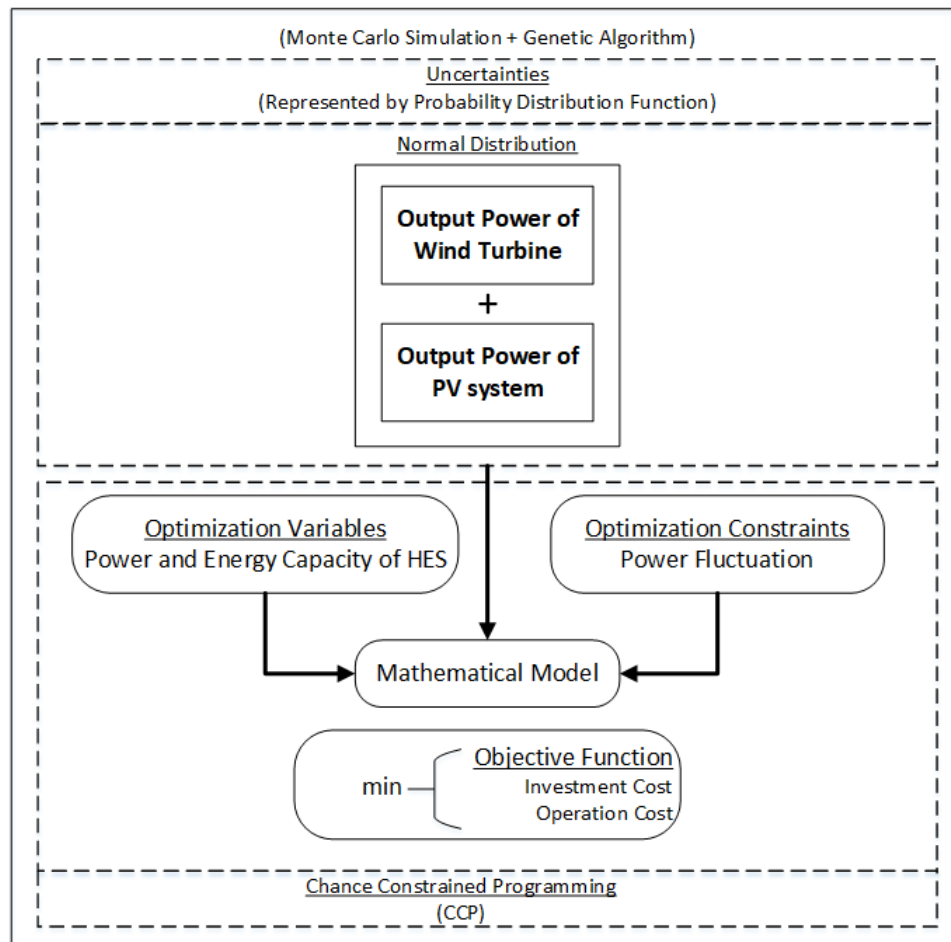
Figure 4.1: Flowchart of the developed CCP-based method for optimal sizing of HES considering uncertainty

### 4.4.3. Sizing HES using CCP-GA optimization

The following assumptions have been made for the optimization procedure:

1.  The uncertainty of wind and solar output power model can be formulated under presumption that the profile obeys a normal probability distribution as followed:

$$\widehat{P}_r(t + k|t) \sim\sim N\left(p(t + k), \sigma(t + k|t)^2\right) \tag{4.32}$$

$$0 \le \widehat{P}_r(t + k|t) \le P_{\text{norm}} \tag{4.33}$$

Where Equation 4.32 introduces a random generator of the fluctuation power $\widehat{P}_r(t + k|t)$ which assumes the next power fluctuation is subject to a normal distribution with the mean of zero and a standard deviation of $\sigma(t + k|t)$. Equation 4.33 ensures the fluctuation power will not exceed the range of installed capacity.

2.  For any given decision of x, using Monte Carlo simulation is used to check the constraint is satisfied. N independent random vectors are generated based on the normal density function, which are $(\xi_1, \xi_2, ..., \xi_N)$. If N is the number of all vectors, then the number of cases that follow or satisfy the constraint 4.31 can be denoted as N'. Mathematically, a chance constraint can be expressed by Equation 4.31 if $\frac{N'}{N} \ge \alpha$.

The goal of the optimization problem is to minimize the overall total cost of hybrid energy storage

while keeping the differences between the actual renewable power otuput and the allowable power profile within a certain limit.

The objective function formulation has been explained in 4.13 and can be described again as follows:

Main steps of this method can be summarized as follows:

$$minC = C_{P,b}P_b + C_{E,b}E_b + C_{P,sc}P_{sc} + C_{E,sc}E_{sc} + \sum_{t}^{T/\Delta t} P_{cur}(t) \tag{4.34}$$

The constraints of the problem are described as follows:

$$s.t. \Pr\{|\Delta P_t| - 10\% \text{ of Total Capacity} \leq 0\} \geq \alpha\% \tag{4.35}$$

$$SOC_{\min} \leq SOC_{t,s} \leq SOC_{\max} \tag{4.36}$$
$$\forall t \in T, \forall s \in S$$

$$\text{if } P_t^{Batt} \geq 0 \text{ or } P_t^{SC} \geq 0 \tag{4.37}$$

$$SOC_{(t+\Delta t),s} = SOC_{t,s} + \eta^{ch}\Delta t P_{t,s}^{Batt/SC} \tag{4.38}$$

$$\forall t \in T, \forall s \in S \tag{4.39}$$

$$\text{if } P_t^{Batt} < 0 \text{ or } P_t^{SC} < 0 \tag{4.40}$$

$$SOC_{(t+\Delta t),s} = SOC_{t,s} - \frac{1}{\eta^{dch}}\Delta t P_{t,S}^{Batt,SC} \tag{4.41}$$

$$\forall t \in T, \forall s \in S \tag{4.42}$$

MC simulation based genetic algorithm optimization is used to solve the CCP-based problem as formulated in constraint 4.35. The penalty function is incorporated into the GA fitness function as the violation of the power fluctuation exceeding the constrained value. The step-by-step optimization procedure can be described as follows:

1. Initialize the algorithm parameters, including power and economic parameters, specify the confidence level of the chance constraint.

2. Input the optimization parameters in the genetic algorithm, including the maximum number of generations (50), and the probabilities of crossover (0.1) and mutation (0.01).

3. Generate wind and PV output power scenarios by MC simulation and initial population of decision variables. In this research, the decision variable (chromosome) used to solve the optimization problem with GA is composed of T genes, or the total amount of hour t in the simulation time window. Each gene represents the amount of charging/discharging power of the hybrid energy storage that is necessary to balance the difference between actual power output from PV and wind turbines, with the admissible power fluctuation.

   Figure 4.2 shows the structure of chromosomes that represent the decision variable in this optimization problem. In each population, charging/discharging state of the hybrid energy storage is generated.

   The amount of balancing power is generated and the positive / negative sign represents the state of charging/discharging of the hybrid energy storage considering uncertain parameter values.
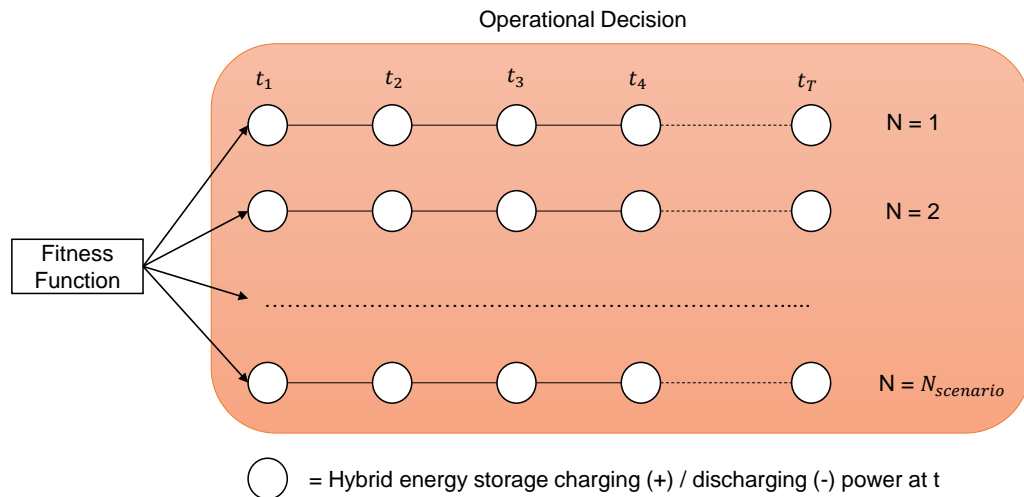
Figure 4.2: Charging or discharging power of the hybrid energy storage in each minute t

According to the power sharing strategy in Section 5.2, the charge/discharge power of both battery and supercapacitor can be determined.

For each given chromosomes, Monte Carlo checks whether the chance constraint is violated or not by the following procedure :

(a) Set a number of simulations allowed (N).

(b) Set counter t = 0.

(c) Initialize N' = 0.

(d) For each t, a random number is generated obeying the normally distributed power fluctuations by using 4.32 and 4.33.

(e) Check whether the chance constraint of 4.35 is satisfied, if yes, set N' = N' + 1.

(f) Set t = t + 1.

(g) If t<T, the iteration starts again from step d, otherwise continue to the next step.

(h) When $\frac{N'}{N} \geq 80\%$, the chance constraint 4.35 is satisfied and return "YES"; otherwise return "NO".

4. Evaluate the objective function to all chromosomes. If the constrains are violated, calculate the fitness function using the penalty function approach based on the objective function. If the chance constraint is not met, it means an amount of wind and PV output power is curtailed, which decreases the fitness calculation as a form of penalty or curtailment factor.

5. Apply selection, crossover, and mutation operators to generate new population generation.

6. Repeat until the given iteration step is reached or termination condition is satisfied. After 5-th generation, the mean average fitness function of the previous 5 generations are compared with the fitness afterwards. If the next average fitness is better, the sampling continues. As GA is a computationally extensive optimization, the defined stopping criterion is when there is no improvement in the population after 5 number of iterations.

## 4.5. Conclusion

This chapter provided an overview of a stochastic approach to analyze the required storage capacity of a hybrid energy storage. Since there are uncertain variables, uncertain programming should be adopted

to solve it. CCP is ensuring that the combined power output from PV, wind turbines and hybrid energy storage match the expected profile of grid acceptable power within the desired level. The Monte Carlo simulation is used as a scenario generation method that provides a general approach for solving CCP problems. Hence an essential demarcation is established between the two methods. CCP is employed in conjunction with a GA optimization problem, and Monte Carlo method is just a form of simulation technique as an alternative way for handling different kinds of uncertainties.

# 5

# Simulation results and discussion

*In this chapter, the details of the power fluctuation of the selected power system is firstly explained. The detailed explanations can be found in Section 5.1. The necessity of installing energy storage to fill renewable energy variability will be described in Section 5.2, by adopting the power sharing management to the hybrid energy storage. Lastly, Section 5.3 broadly explained the evaluation of cost-based optimization of the hybrid energy storage and comparisons of different technologies.*

## 5.1. Grid Power Fluctuation

This research uses the real 365-days of wind and PV data from a 5 kW wind farm and 7 kW of solar array in Indonesia to test the performance of the proposed method. According to Equation 3.8, the maximum fluctuation of the power output is 1,2 kW for each minute. Figure 5.1a and 5.1b show the original power output and the grid acceptable power according to the standard, obtained by using Equation 3.2 to 3.8. The acceptable power output can be denoted as the power injected into the grid after combining the actual power output with the hybrid energy storage power charge/discharge output power.



(a) 24-hour interval
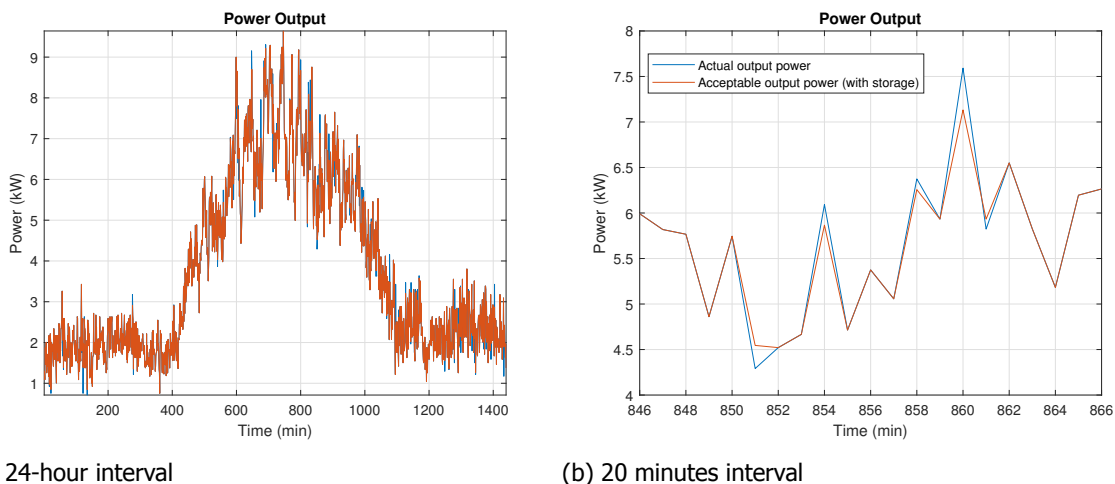(b) 20 minutes interval

Figure 5.1: Grid acceptable power with 1 minute timescale

To meet the requirement of the grid acceptable power standard, HES is applied to maintain the balance between the grid input power and the output power from wind turbine and PV array, which

will result in the orange line. The algorithm is proven able to obtain the grid acceptable power as illustrated in Figure 3.3, where the power injected to the grid is automatically corrected its value when the fluctuation value is beyond the range of ±1,2 kW.

The difference between the original power output and the acceptable power output represents the balancing power, as shown in Figure 5.2. FFT method according to Section 3.2.3, is conducted to the balancing power to convert the signal from time domain into frequency domain as shown in Figure 5.3.
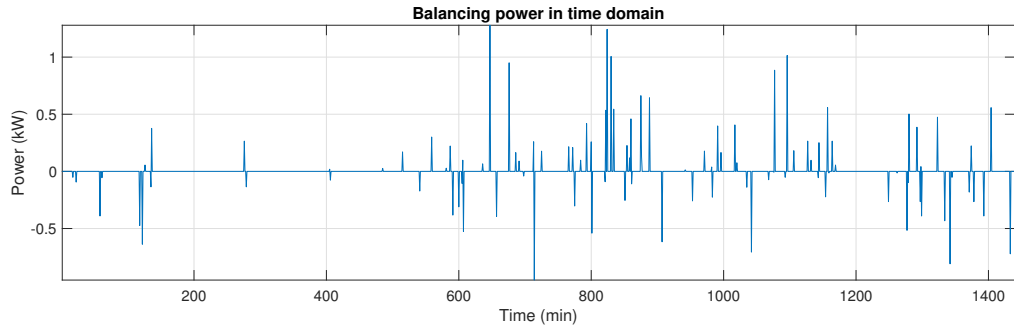


Figure 5.2: Balancing power in time domain
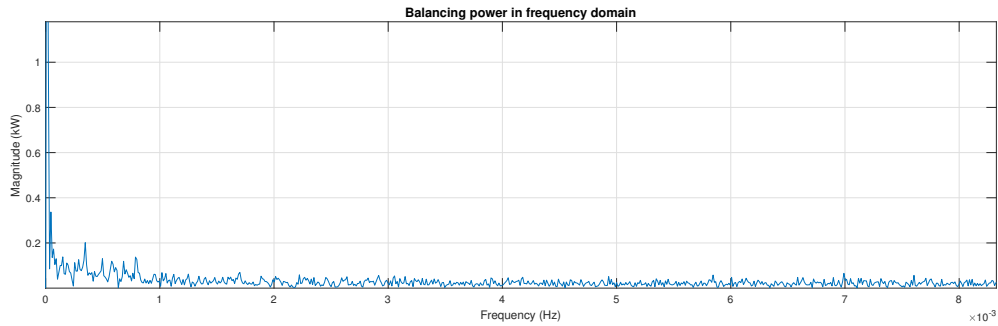


Figure 5.3: Balancing power in frequency domain after FFT method

From the frequency domain, it can be seen that most of the spectrum of balancing power is concentrated on the low frequency part. The low frequency balancing powers are of high amplitudes when compared to the high frequency balancing powers. Even though the amplitudes are much lower than the low frequency components, high frequency components existence will still affect the overall energy storage capacity if only one energy storage type is applied in the system.

Table 5.1: Power and energy capacity of battery-only storage system

|                              | Rated Power (kW) | Rated Capacity (kWh) |
|------------------------------|------------------|----------------------|
| Battery-only storage system  | 1.6              | 6.4                  |

Table 5.1 shows that if a battery-only energy storage system must satisfy the total balancing power in Figure 5.2, its rated power and energy capacity will be oversized a lot. Moreover, if only battery is to compensate the high-frequency components contained in balancing power, the capacity configuration is expected to be oversized. Consequently, total investment and operation cost will increase. Therefore, implementing a hybrid energy storage which consists battery and supercapacitor technologies is proposed. The supercapacitor is in charge for all the high-frequency transients of the balancing power. On the other hand, battery technology is accountable for all slow-variation signal from balancing power. The energy of high-frequency components can be absorbed which not only will smooth the actual output power from the renewables, but also will reduce the capacity of battery energy storage and the total cost of operating the system.

## **5.2.** Power Sharing Management of the HES

In mathematics, the wavelet is a sequence of square-shaped functions that contains different scale. The analysis of transforming balancing power with wavelet method begins with a decomposition of the balancing power signal into an approximation and a detail sequence, as shown in Figure 3.6. Balancing power from Figure 5.2 is considered as the original input data for the wavelet analysis, f(k), for k = 0, T, 2T,..., (N-1)T; where T is the sampling time. Sampled signals are denoted as finite sequences of numbers, for example, $f_1$, $f_2$, and so on. Wavelets are defined by the wavelet function and its scaling function in the time domain. Transforming sequences ($f_k$) to a continuous-time signal f(t) be obtained by using "scaling function", to construct each wavelet as shown in Equation 3.17.

The basic idea of this wavelet transform is to replace an adjacent pair of steps by one wider step and one wavelet. As an example, consider the following sampled signal which has a length of 8 and consists of:

$$f = \{f_k\}_{k=0}^{7} = \{8, 4, 6, 8, 9, 7, 2, 4\} \tag{5.1}$$

Figure 5.4 represents the sequence signal $f_k$ and its wavelet function, constructed using the scaling function by using Equation 3.17. Therefore, the continuous-time signal f(t) is a piecewise constant on intervals of length one.
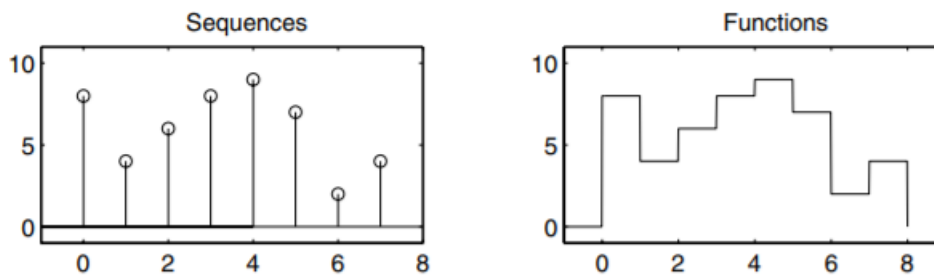


Figure 5.4: Sequence (left) signal and wavelet function (right) signal of f

A "coarser version" of $f^1$ of the sequence $f$ can be computed by calculating the mean of neighboring sequence elements, as shown in Equation 5.2.

$$f^1 = \{f_k^1\}_{k=0}^{3} = \left\{ \frac{f_0 + f_1}{2}, \frac{f_2 + f_3}{2}, \frac{f_4 + f_5}{2}, \frac{f_6 + f_7}{2} \right\} = \{6, 7, 8, 3\} \tag{5.2}$$

The result of combining two neighboring steps with width 1 into one step of width 2, leads to a power signal $f^1$ that contains half of the length of the original signal $f$. $F^1$ = 6,7,8,3 represents a coarse approximation of the initial signal $f$. The first half of the sample, (8,4), has an average value of (6), and so does for the rest of the sample. Afterwards, the continuous-time signal f(t) can be constructed by using Equation **??** with intervals of length 2. $F^1$ is a new sequence signal which again is used to construct the corresponding wavelet function $f^1(t)$, likewise a piecewise constant signal but with intervals of length 2 as shown in Figure 5.5.

After obtaining the coarsened signal, the detail signal can be obtained by calculating the difference signal between $f(t)$ and $f^1(t)$. The "detail signal" represents the signal contributions that are necessary to recover the coarsened version of signal $f^1(t)$ to the original signal $f(t)$.

This signal also is called "detail signal". Detail signal by definition represents the signal contributions which are needed to recover the original signal f(t) from the coarsened version $f^1(t)$. After computing
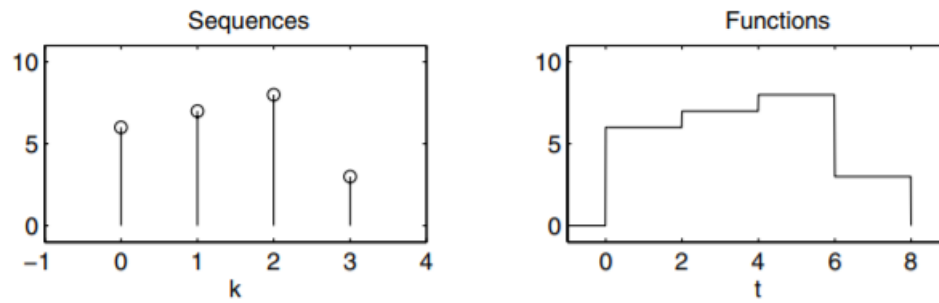
Figure 5.5: Sequence (left) signal $f^1$ and wavelet function (right) signal of $f^1(t)$
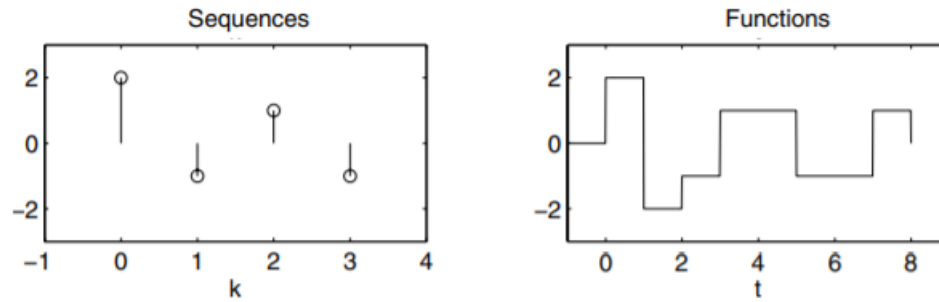


Figure 5.6: Sequence (left) signal $d^1$ and wavelet function (right) signal of $d^1(t)$

the sequences of $d^1$, the continuous-time signal of $d^1(t)$ can be constructed as shown in the right-side of Figure 5.6.

The above procedure is a one-step-version of the wavelet transform, which is applied to the rest of the original balancing power. The computation of $f^1$ can be described as :

$$f^1 = Hf \tag{5.3}$$

where H represents the downsampling of the signal, where the number of sequence elements are divided by two. Later on, the difference between original signal and the downsampled signal, $d^1$, can be written as:

$$d^1 = Gf \tag{5.4}$$

where $d^1$ represents the details needed to recover f, and G represents the upsampling of the signal that is used to double the width of $f^1$ as a consequence of the coarsening procedure. This following formulas are extended to a general discrete signal of length N, which in this case, the balancing power to smooth the renewable power fluctuation. The representation of the complete procedure is illustrated in Figure 3.5.

According to Equation 3.20, the maximum decomposition layer of three is used here. The three-level wavelet transform is utilized for decomposition of the balancing power as shown in Figure 5.2. Ultimately, the power signal decomposition is used to obtain the transients that can be assigned for the supercapacitor. Figure 5.7, 5.9 and 5.10 represent the approximation signals which contain the low frequency components of the original balancing power signal. For display purposes, results are displayed with time-scale of one day.

Figure 5.7 is obtained by replacing neighboring pair of sequences by one wider step and one wavelet,
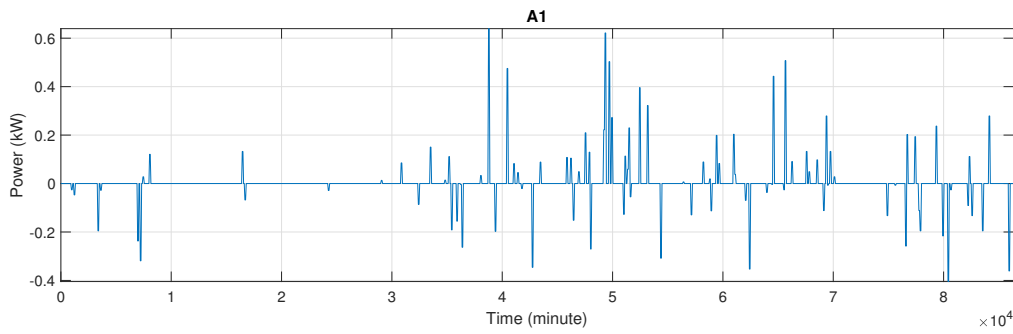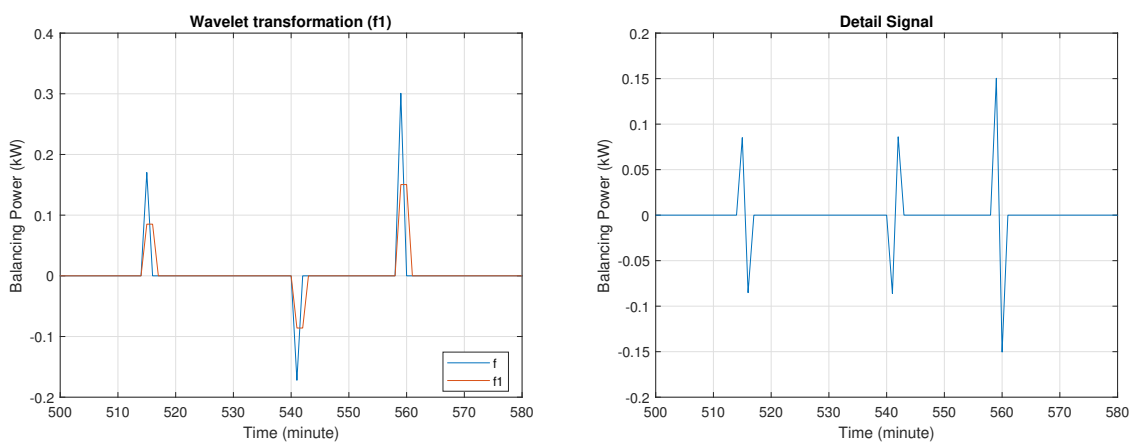
Figure 5.7: Approximation Signal Level-1

following Equation 5.2. A zoomed-in version of the signal ($f(t)$) and its wavelet functions ($f^1(t)$) are illustrated in Figure 5.8a and 5.8b.



(a) $f(t)$) and $f^1(t)$



(b) Difference signal of $f(t)$ and $f^1(t)$

Figure 5.8: f, $f^1$, and $d^1$ signals

The wavelet transformation is repeated by using the newer sequence $f^1$, or the approximation signal level-1 in Figure 5.7. With each decomposition process, the (n+1)-th level approximation signal expresses the sum of a new, coarser approximation and a new, lower-frequency set of wavelets from the previous level.
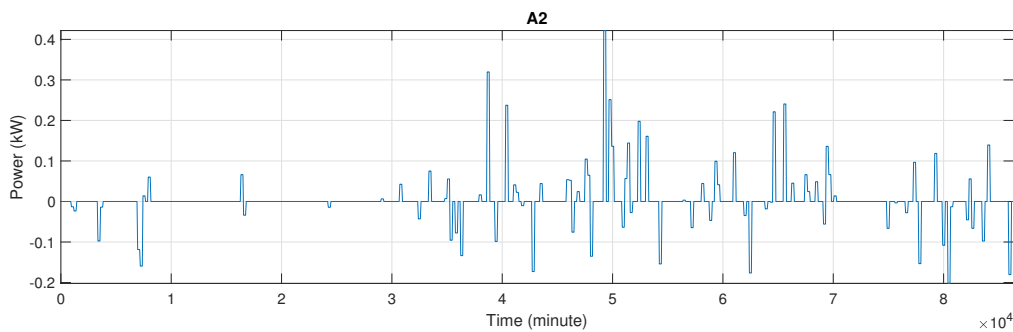


Figure 5.9: Approximation Signal Level-2

After three-level decomposition processing, the last approximations signal which contains low-frequency signal is extracted from the total balancing power x(n) as the power demand for the battery system, as shown in Figure 5.10. Peak power of each approximation signal also reduces accordingly, from 0.65 kW to finally 0.21 kW. An essential understanding from the reduction of the peak power is
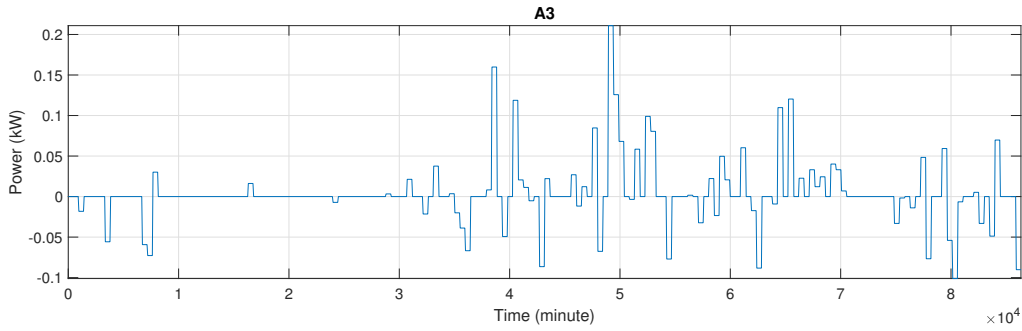
Figure 5.10: Approximation Signal Level-3

that the wavelet power decomposition can separate between true components and the noise in the original power signal. The reduced peak value refers to interference or noise signal, which will be absorbed by the supercapacitor to smooth the power curve.

The method can distinguish the transients, which forms the detailed signals that only contain high-frequency components. The transients, $[D_1(n), D_2(n), D_3(n)]$ are distributed to the supercapacitor, which resulting in power demand for the device as the total sum of high-frequency signals shown in Figure 5.11, 5.12, and 5.13.
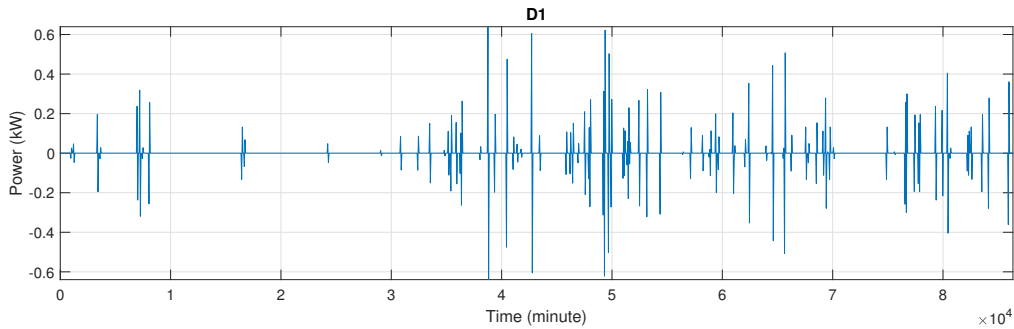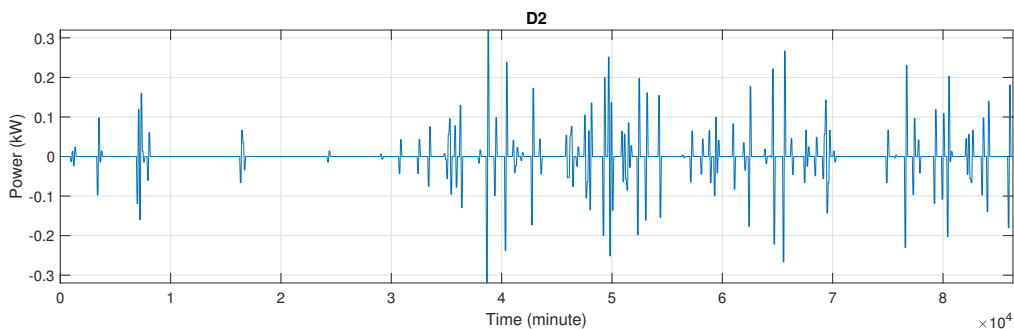


Figure 5.11: Detail Signal Level-1



Figure 5.12: Detail Signal Level-2

Figure 5.7 until 5.13 shows that lower detail components have higher frequencies, which corresponds to the component in the balancing power which rapidly changes and fluctuates heavily up and down near zero. Consequently, the energy of the higher frequency signals is low. On the other hand, the approximation signals have lower frequencies, with slowly changing component of the balancing power. A3 in Figure 5.10 represents the slowest changing component of the whole power spectrum in the balancing power. The low frequency A3 can be distinguished as the main part of the original balancing power curve, thus play a dominant role.

Figure 5.14 shows the zoomed-in decomposition process of the original balancing power signal
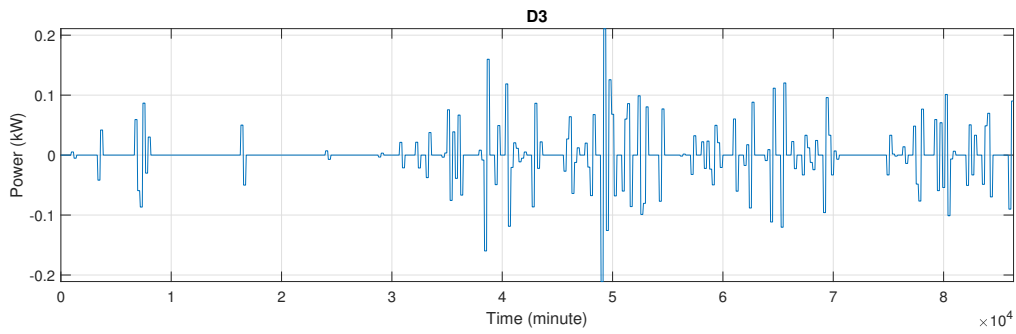
Figure 5.13: Detail Signal Level-3

into approximation component and detailed component by wavelet transform. According to the different power and energy density characteristics of the two types of the mentioned storage devices, the detailed part which contains a lot of high frequency components, is suitable to be compensated by supercapacitor. On the other hand, the majority of approximation part is convenient to be met by battery system. The strategy can successfully segregate balancing power into low- and high-frequency components.
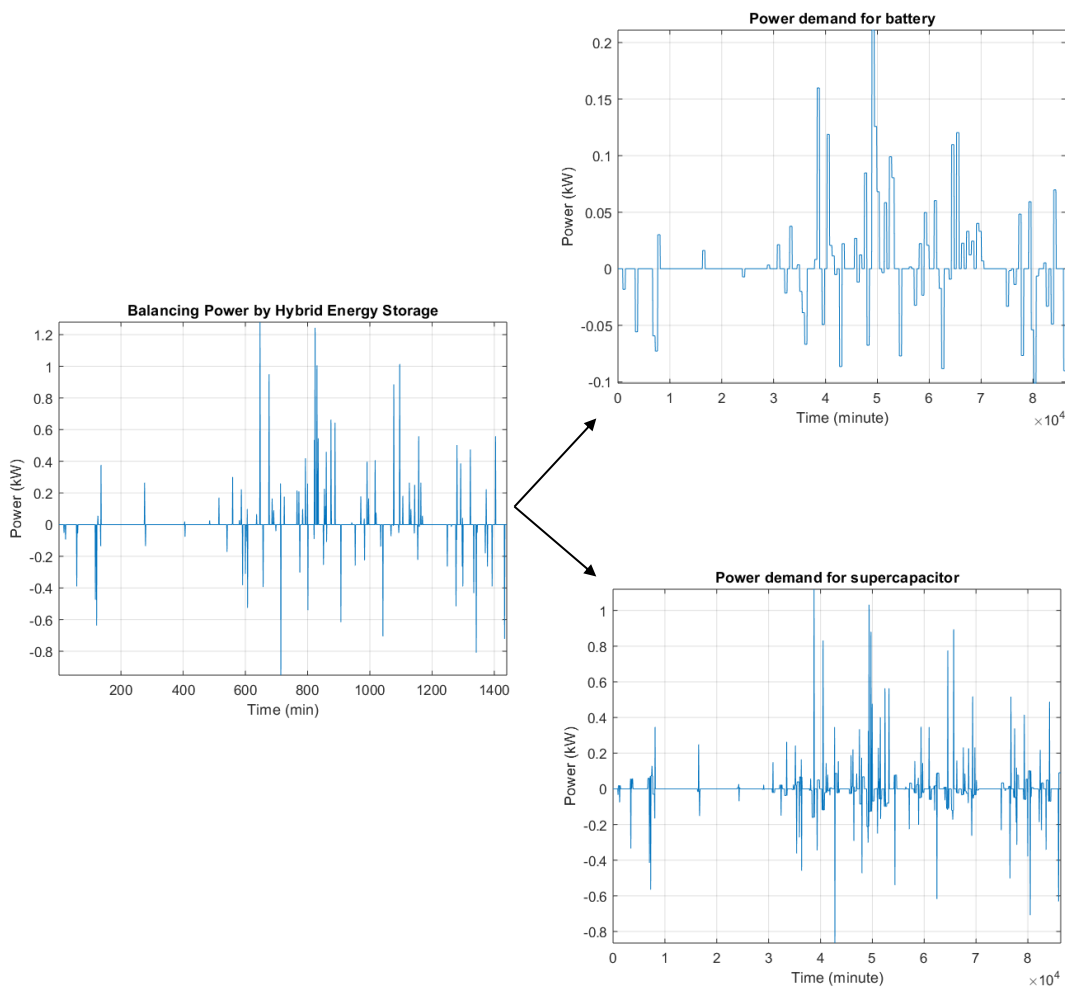


Figure 5.14: Zoomed-in decomposition of balancing power using wavelet transform

It can be observed from the results of power sharing using the wavelet decomposition in Figure 5.14, the power demand for battery does not contain high frequency components anymore. The peak

power that the battery faces is reduced from 0.64 kW to 0.2 kW, in addition to the slower power derivative. The power demand curve for battery after wavelet decomposition is complementary with the slower response speed characteristics of battery technology. On the other hand, the total of all detailed signals are supplied by the supercapacitor, supplying 1.1 kW of peak power to the grid.

The supercapacitor power, shown in Figure 5.14, is the detail part of the balancing power and consists of transients, which is appropriate for the device's characteristics. The high transients are compensated, providing up to 1.2 of peak power and relieving the burdens on the battery system. The power demand curve for supercapacitor has low energy but changes quickly, which is complementary with the characteristics of supercapacitor that has faster response speed compared to battery technology.

Table 5.2 shows the energy and power capacities of both battery and supercapacitor after the power sharing management by wavelet analysis decomposed the balancing power to smooth out the fluctuation on the grid. It is important to mention that the combined smoothing output in this case met the overall systems fluctuation constraints to the maximum event, which in this case represents a 100% confidence level.

Table 5.2: Energy and power capacities of the HESS after wavelet transformation

|                    | Battery | Supercapacitor |
|--------------------|---------|----------------|
| Rated Power (kW)   | 0.3     | 1.2            |
| Rated Capacity (kWh)| 5.8    | 0.5            |
| SOC range (%)      | 20 - 80 | 5 - 95         |

Table 5.2 shows that the battery system energy capacity is relatively larger than the supercapacitor energy capacity. Compared to the battery-only storage in Table 5.1, rated power of battery in hybrid energy storage with using wavelet power sharing method reduced from 1.6 kW to only 0.3 kW. Moreover, rated capacity of battery also decreased from 6.4 kWh to 5.8 kWh for battery-only storage system and battery in the hybrid energy storage system respectively.

Figure 5.15 shows that with the increase of confidence level, the energy capacity of both battery and supercapacitor is increased. There are two turning points, 84% and 98%, which will be investigated. With only 84% of confidence level in smoothing the power fluctuation, battery with a capacity of 2 kWh and supercapacitor with a capacity of 0.2 kWh is needed. On the other hand, a battery capacity of 4 kWh and a supercapacitor capacity of 0.3 kWh is necessary to deal with 98% of all the fluctuation.
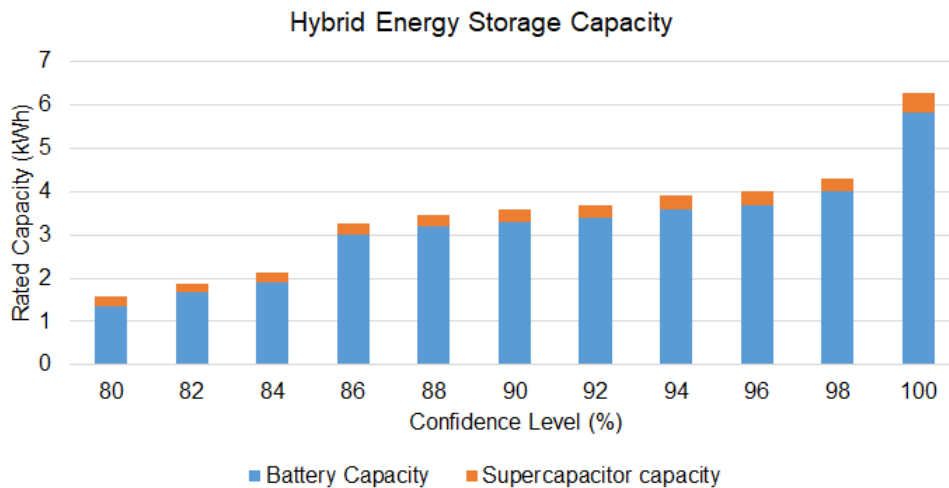


Figure 5.15: Hybrid energy storage capacity under different confidence levels

It can be seen from Figure 5.16a and Figure 5.16b that capacity of energy storage is a key factor for the operation strategy and optimal result of power smoothing. If the hybrid energy storage capacity is

adequate, the smoothing effect of the actual power output can be obtained. However, with a difference of 2 kWh in the battery capacity between 84% and 98% confidence level, several peaks are not handled by the hybrid energy storage, which will result in power curtailment.
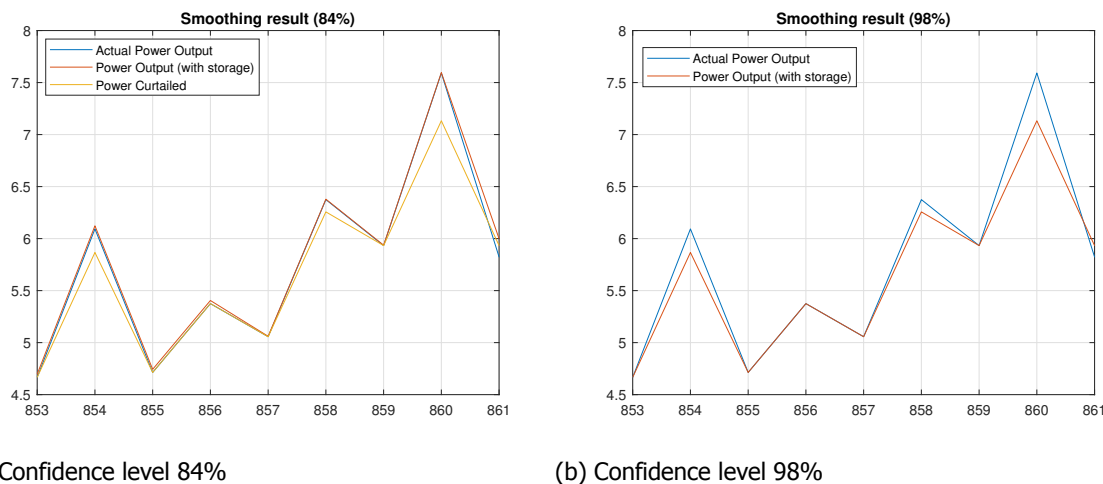


(a) Confidence level 84%                                  (b) Confidence level 98%

Figure 5.16: Result of smoothing fluctuation operation strategy under different confidence level

Peaks at t= 854, 858 and 860 minute show that there is no power smoothing effect from the hybrid energy storage. Inadequate sizing of the energy storage under 84% confidence level causes limited allowable charge/discharge power that can be fed to the grid to handle PV and wind power output fluctuation. Consequently, the amount of difference between actual power output and acceptable deviation is curtailed, which also has an effect on the systems operation costs that will be broadly explained in Section 4.2.3.

## 5.3. Optimal Sizing of HES

The algorithm is provided along with the effective power sharing strategy of battery and supercapacitor to obtain the optimal capacity of hybrid energy storage to smooth the PV and wind output power fluctuations. The optimal total cost will be investigated through the capital cost in Section 5.3.1, operating cost in Section 5.3.2 and replacement cost in Section 5.3.3 through out the lifetime of the energy storage system. Ultimately the optimal toal cost of hybrid energy storage technology considering renewable energy uncertainty is identified in Section 5.3.4.

### 5.3.1. Capital cost

During the objective function evaluation of the population, the final values are recorded and compared. From Figure 5.17 it can be observed that GA optimization is able to reach a constant value at the ninth iteration. The iteration is terminated after the 13-th iteration when the local minima of the objective function is not changing

Figure 5.18 shows the total capital cost rises as the confidence level increases from 80% to 100%. For the confidence level of 80% to 98%, the cost curve rises slowly. However, with an increase in above 98%, it is observed that it contributes to a higher degree of total investment cost. With only 2% increment, the price escalates quickly for almost 49% of the from 13230$ to 19437$, with almost 47% of the increase. Despite the gradual increase, there are several sharp rises between the interval of 84-86% and 92-94%, with a total increment of 22% and 10% respectively. On the other hand, other intervals show less than a 10% increase.

As mentioned in Section 5.3.1, the total capital cost is a one-time expense incurred on the purchase
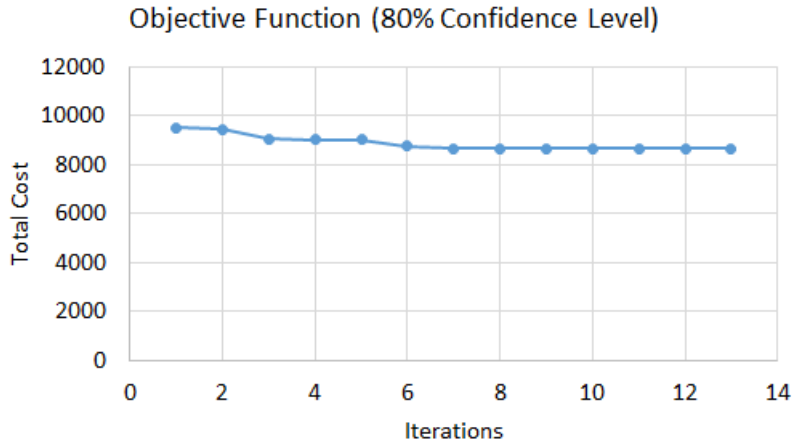
Objective Function (80% Confidence Level)

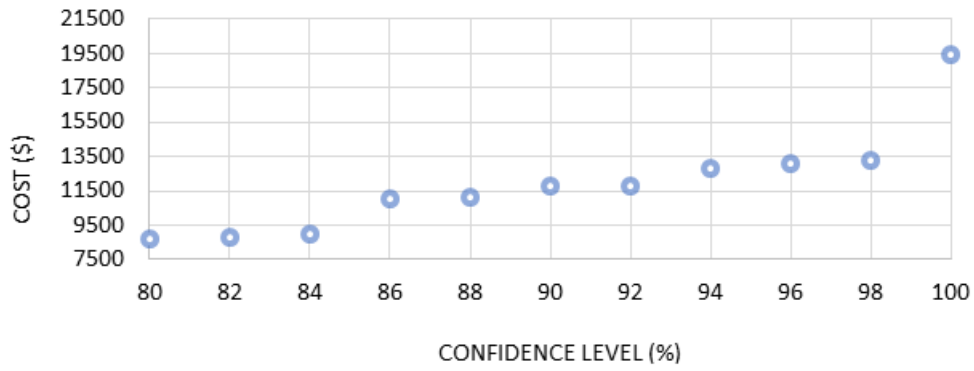Figure 5.17: GA optimization objective function plot

Figure 5.18: Total cost of HES under different confidence levels

of the whole energy storage components, consists of unit capacity and the unit power cost of the battery and supercapacitor. Increase in the confidence level contributes to higher capacity of both devices. Table represents the rated capacity and power of storage battery and supercapacitor for confidence intervals, which has a steep increment in the total capital cost.

Table 5.3: Energy and power capacities of the HES under different confidence level

| Confidence Level | Battery | | Supercapacitor | |
|---|---|---|---|---|
| (%) | Prated (kW) | Erated (kWh) | Prated (kW) | Erated (kWh) |
| 80 | 0.15 | 1.37 | 0.94 | 0.21 |
| 86 | 0.2 | 3.3 | 1.1 | 0.25 |
| 94 | 0.27 | 3.6 | 1.18 | 0.3 |
| 100 | 0.3 | 5.8 | 1.2 | 0.46 |

Table 5.3 shows that the rated power and capacity of battery and supercapacitor under different confidence level. The result shows that to completely cover the whole range of uncertainties, hybrid energy storage power and energy capacities are necessarily much higher than the expected value capacities. However, if a certain level of risk is acceptable, both power and energy capacities will become considerably smaller and the model allows this risk estimate.

Figure 5.19 represents the composition of the investment cost of hybrid energy storage compared to the battery-only storage system. The optimal supercapacitor sizing has a significant contribution to the overall capital cost. The one-time expenses rapidly increased with increasing supercapacitor capacity. Consequently, the capital cost for a battery-only energy storage system is far more affordable
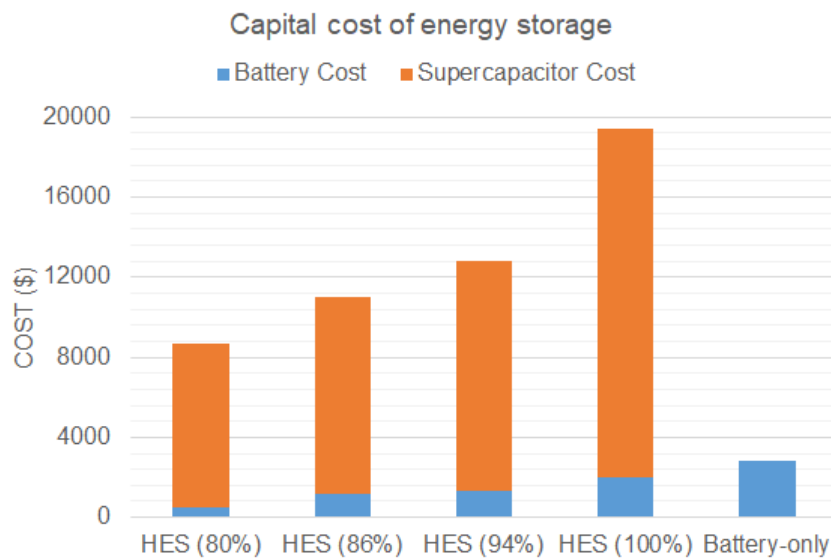
compared to installing hybrid energy storage.



Figure 5.19: Investment cost of HES under different confidence levels

The study of using hybrid energy storage system was initially developed to improve the smoothing of power fluctuation on the grid while improving the battery's lifetime and replacement cost. When only looking at the capital cost, the advantages of using hybrid energy storage in an electrical power grid are weakened, as the cost difference between them is too significant. Moreover, battery's cost is also declining in the future, making the hybrid energy storage more unfavourable. Therefore, including operation and life cycle cost calculation is necessary to have a better comparison between hybrid energy storage to that of the battery-only energy storage system, and clearly, show the advantages of adding the supercapacitor.

### 5.3.2. Penalty / Occurring cost

The present value of the penalty cost of a hybrid energy storage system is the present value of all penalty costs occurring in 10 years, which is the expected total system lifetime. Penalty costs are applied to the accumulated solar and wind energy that needs to be curtailed or in deficit. Consequently, the penalty cost will reduce the economic benefits of integrating solar and wind power generation into the system.
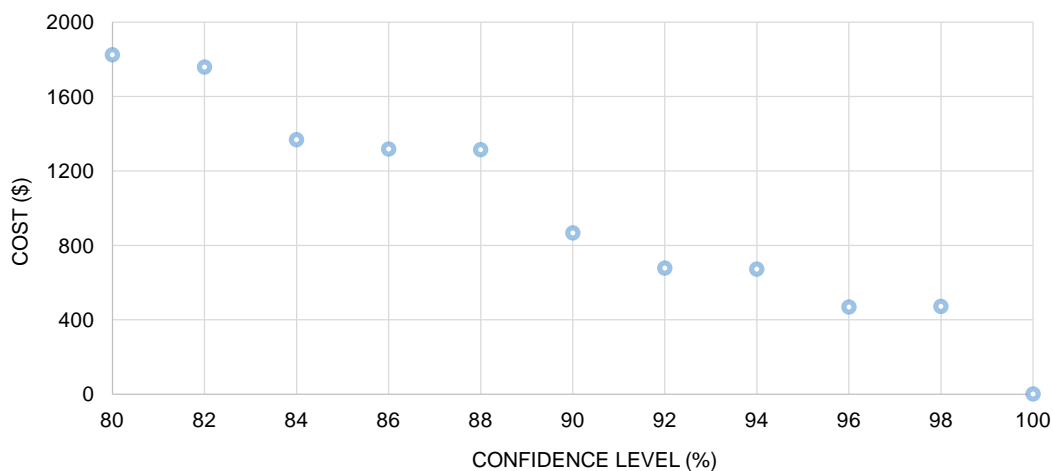


Figure 5.20: Penalty cost of HES under different confidence levels

Figure 5.20 displays the total penalty cost imposed on power producers if the total output from PV and wind turbines exceed what the grid can accept. The result shows that with a low confidence level of the hybrid energy storage, less penalty cost is incurred to the power producer. With the optimal configuration of hybrid energy storage being under a confidence level of 90%, more than 1000$ of penalty costs over ten years of the system's lifetime. Over period of 10 years, using a HES under 100% confidence level does not impose any penalty to the power producers.

Figure 5.21 represents the battery state of charge respectively under 80% confidence level. The SOC of battery is kept in the range between 0.2 and 0.8 in order to prevent overcharging/discharging. It can be seen that under confidence level of 80 %, battery reaches the maximum level of their SOC, resulting in curtailment of the PV and wind power output.
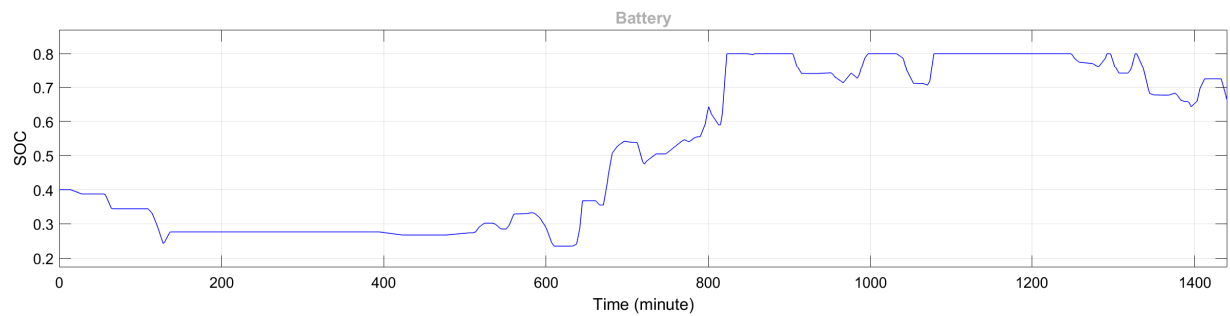


Figure 5.21: SOC Battery (80%)

Most of the time, curtailment losses come from power from PV and wind turbines that is not exported to battery nor the grid and cannot be used. Table 5.4 shows that higher confidence level, implies to higher capacity of both battery and supercapacitor, can reduce the curtailment losses and maintain the state of charge within the safe range.

Table 5.4: Power curtailed under different confidence level

| Confidence Level (%) | Power Curtailed (kW) |
|---|---|
| 80 | 2642 |
| 82 | 2387 |
| 84 | 2319 |
| 86 | 1369 |
| 88 | 1153 |
| 90 | 1019 |
| 92 | 917 |
| 94 | 651 |
| 96 | 527 |
| 98 | 280 |
| 100 | 0 |

It is worth to mention that the curtailment is associated with investments of the hybrid energy storage, where power producers voluntarily accepts curtailment due to the power grid fluctuation constraint.

### 5.3.3. Life cycle cost

Rainflow algorithm principle as broadly explained in Section 3.2.2 is used to define full and half cycles of battery's state-of-charge in each confidence level. Once the number of cycles are calculated, the rainflow histogram with fixed depth-of-discharge range is created to show the linkage between number of cycles, depth-of-discharge interval and battery's lifetime.

Figure 5.22 shows the comparison of battery-only energy storage and hybrid energy storage lifetime on each confidence level. Based on Equation 3.10, in the case of the battery-only energy storage system, the expected lifetime for the battery is 1.3 years, whereas in the case of hybrid energy storage, battery lifetime is expected to be 6.2 years. By using battery alone as the energy storage system, the battery lifetime is reduced due to compensating all the balancing power.
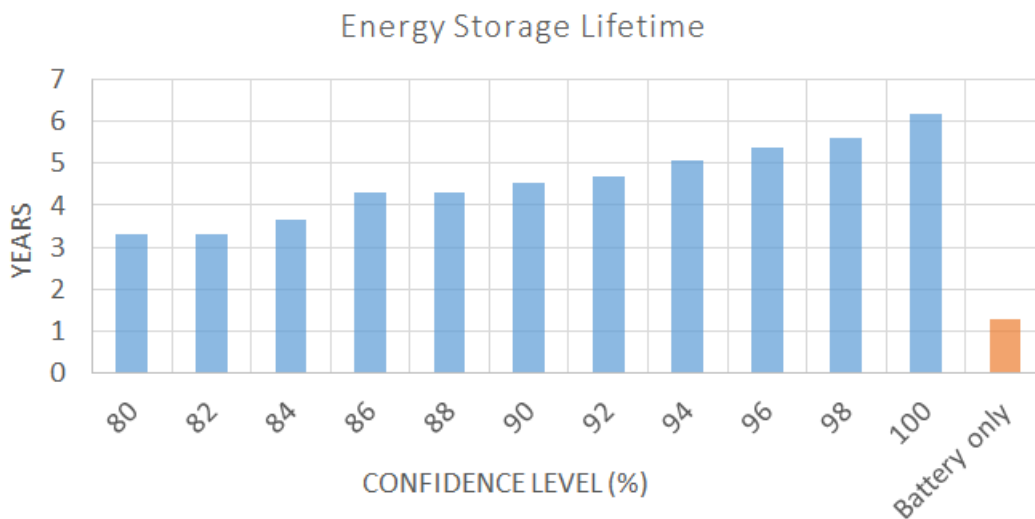


Figure 5.22: Comparison of energy storage lifetime

As shown in Figure 5.23a and 5.23b, the increase of almost 5 years of battery lifetime corresponds to the decrease of 10 discharge/charge cycles per day. By utilizing supercapacitor in the energy storage system alongside the battery, high-power transients in the power fluctuation on the grid can be compensated by charging/discharging the supercapacitor, rather than using power drawn for the battery. Not only the amount of cycle counts, but utilizing supercapacitor also affects the interval of depth-of-discharge. The figures show that the amount of cycle shift towards the low DOD range, from 0.4-0.45 to 0.35-0.4. The result shows that cycling a battery at a lower DOD improves prolong the battery's lifetime.
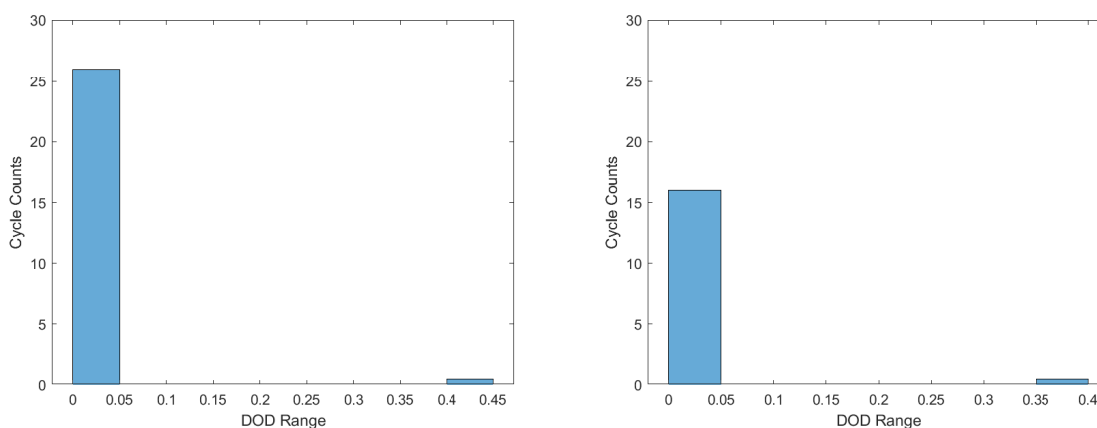


(a) Energy storage with battery only



(b) Energy storage with battery and supercapacitor

Figure 5.23: Histogram of rain-flow cycles results

Figure 5.24a and 5.24b will show more correlation between the number of battery's cycles and its lifetime. The histogram of cycle counts shows a mix of partial and full cycles which can be translated

into a real battery's lifetime. Operating the hybrid energy storage under 86% of confidence level results in 4 years of battery's lifetime, while operating HES under 94% of confidence level increases the lifetime to 5.5 years. The cycle life also shows improvements by having more cycle at reduced DOD range. Figure 3.4 shows that by regularly discharging the battery at a lower DOD interval, the battery will have more useful cycles. On the other hand, frequently discharging the battery a higher DOD range will drain the device. The histogram of rain-flow cycles in Figure 5.23a until 5.24b are aligned with the battery manufacturer's data. Increasing confidence level of smoothing power fluctuation effort in a hybrid energy storage will also increase the capacity of battery. Adequately sizing the battery will avoid rapid charging/discharging modes, as shown in Figure 5.21 and 5.26. Consequently, the charging cycle in the battery is reduced and the battery lifetime is improved.



(a) hybrid 86                                                          (b) hybrid 94
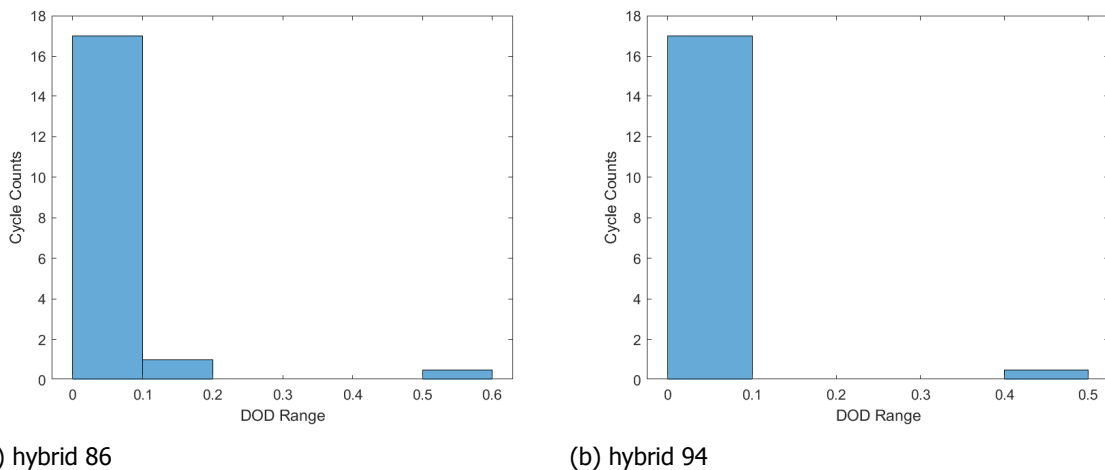
Figure 5.24: Histogram of rain-flow cycles results

Figure 5.25 and 5.26 represents the battery's SOC in a battery-only storage system and in a hybrid energy storage under 100% confidence level. By only using battery in the energy storage system, battery experiences frequent shifts in charging and discharging states. On the other hand, Figure 5.26 shows that battery's state of charge in a hybrid energy storage is relatively more stable with less shift of charge/discharge states. Both SOC curves are not violating the safe operation range of the battery (i.e., 20-80%) as the battery capacity is adequately sized without taking into account the confidence level of smoothing power fluctuation effort.
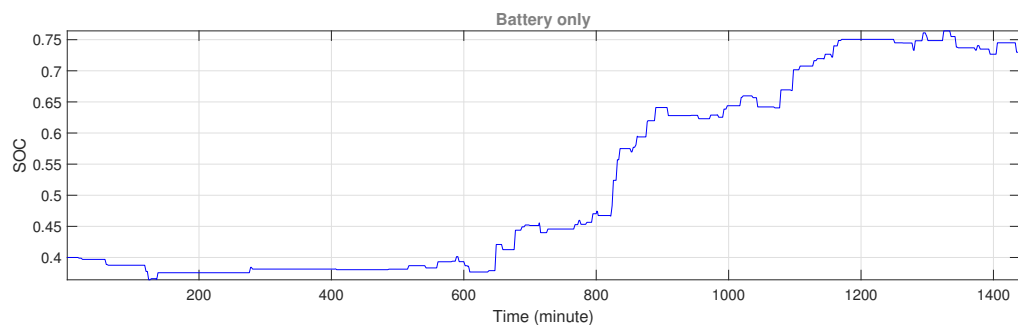


Figure 5.25: Battery's SOC of a battery-only storage system

The state of charge curve validates the linkage between battery's operating condition and its lifetime. If a battery that is not adequately sized, for example under confidence level of 80% in Figure 5.21, is compared to the battery with 100% confidence level of smoothing renewable power fluctuation, the former curve shows violation of the SOC limits while the latter is able to keep the SOC within the safe range. According to lifetime data of battery under each confidence interval in Figure 5.22, battery with confidence level of 80% will only last for 3.3 years, while with 100% confidence in smoothing renewable output power fluctuation, battery will last for 6.2 years. Not only that the battery experienced
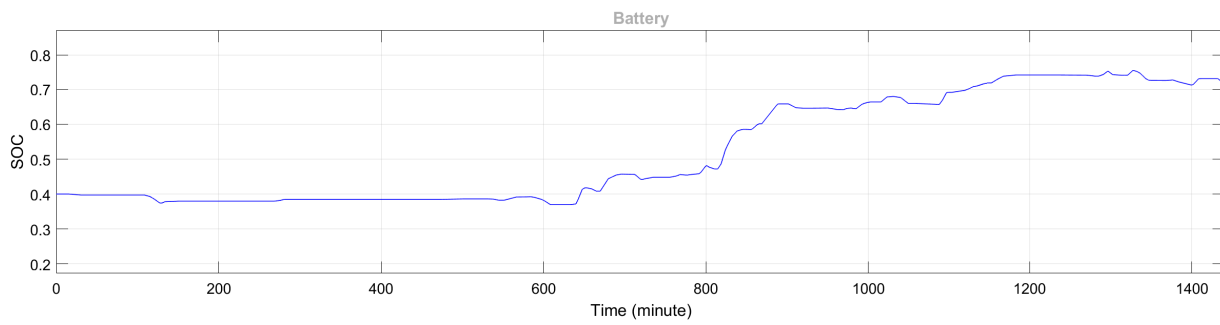
Figure 5.26: Battery's SOC of a HES (100%)

frequent charging and discharging, in the case of 80% of confidence level, battery also experienced over-charging that should be avoided. Therefore, violation of the SOC limits may result in shorter lifetime and early failure. The degradation of the battery is more prominent due to the frequent battery charging/discharging cycles.

Even though in this research it is assumed that supercapacitor will not be replaced over the project's lifetime, it is still worth to investigate the SOC curves of the technology under different confidence level. Figure 5.27 and 5.28 shows the SOC curves of supercapacitor under 80% and 100% of confidence level in smoothing the renewable power fluctuation. The total rated energy of supercapacitor is 0.2 kWh and 0.5 kWh respectively.
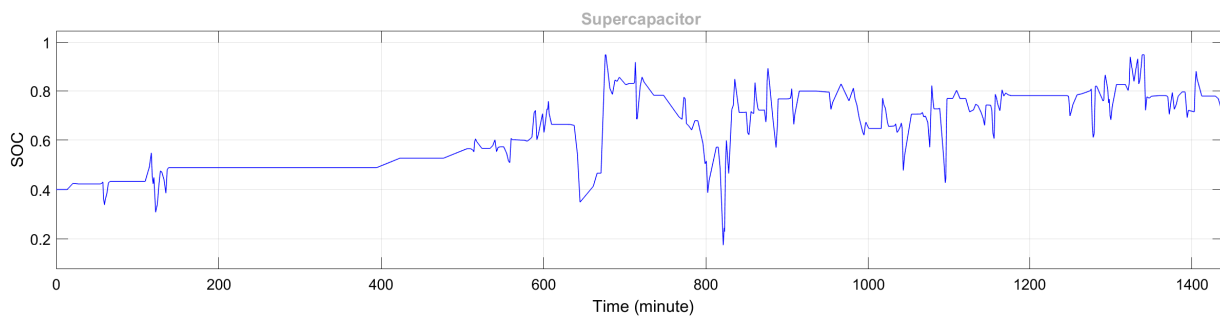


Figure 5.27: SOC Supercapacitor (80%)
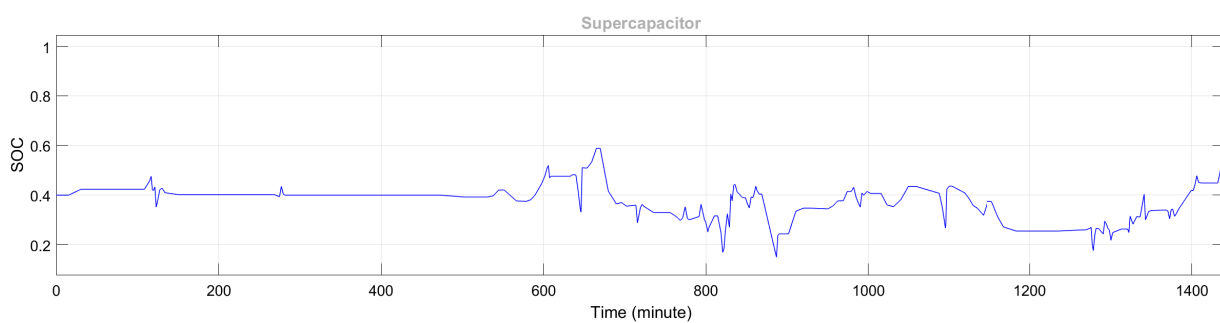


Figure 5.28: SOC Supercapacitor in a HES (100%)

Even though there is no SOC violation (i.e., 5-95%) in both cases, the supercapacitor's SOC curve under confidence level of 80% shows rapid charging/discharging states compared to confidence level of 100%. While the desired capacity configuration of supercapacitor is smaller, installing a 0.2 kWh of the technology causes rapid changes of charging and discharging mode, which may lead to a low lifetime similar in the case of battery energy storage. Adequately sizing the supercapacitor avoids the frequent charging and discharging of the device as seen in Figure 5.28.

### 5.3.4. Total cost of optimally sized hybrid energy storage

Section 5.3.1 until 5.3.3 has identified all cost components that form the objective function of the sizing capacity of hybrid energy storage. Figure 5.29 presents the total cost of energy storage worth of investment, operation and life cycle cost. The final cost results estimates the future spending that includes the inflation and interest rate to consider the time-value of expenditure for 10-years of project lifetime.
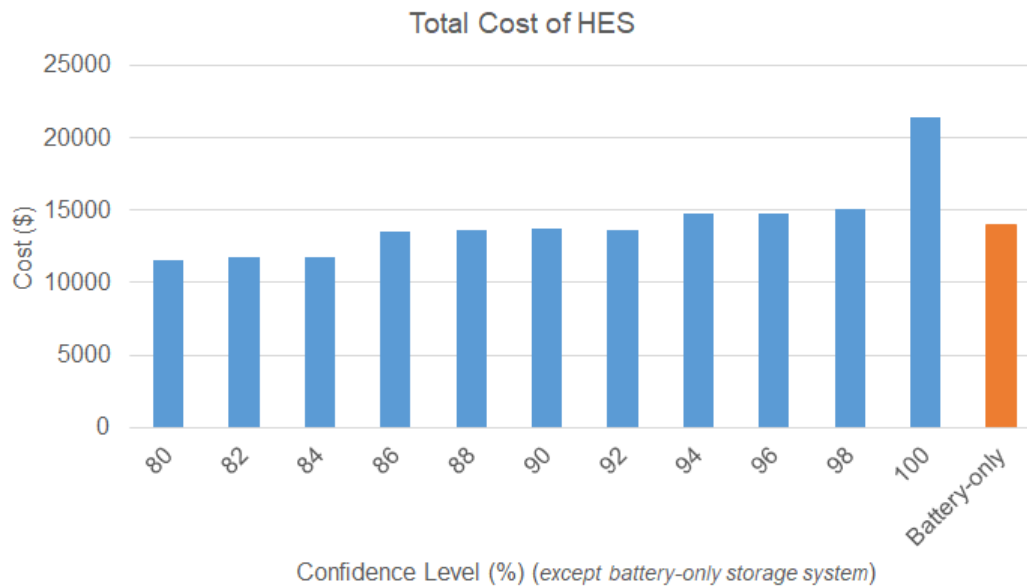


Figure 5.29: Total cost of energy storage

The HESS equipped with battery and supercapacitor energy system shows that the investment is suitable to replace the traditional battery energy storage system. A hybrid energy storage with up to 90% confidence level in handling the power fluctuation is more economically feasible compared to the total cost of using a single battery energy storage device, which is 13979$. The 10% reduction in cost, along with better battery lifetime and performance using a hybrid energy solution, shows that 1.7281 kWh of battery energy storage and 0.026 kWh of supercapacitor the optimal size of HES.

Figure 5.30 shows the comparison of total cost of hybrid energy storage with total penalty cost over the system's lifetime without adding any energy storage into the system. The result shows that with hybrid energy storage which operate under an 80% confidence level, the total cost of adding battery and supercapacitor can compete with the cost of curtailment. Smoothing power volatility with a hybrid energy storage under confidence level of 80% results in 1.37 kWh and 0.2 kWh of energy capacity for both battery and supercapacitor respectively.

Findings from multiple researchers and articles show that curtailment of renewable energy may be cheaper than investing in a grid-scale energy storage system. In some cases, curtailment of low-cost solar and wind can still produce energy below the variable cost of burning natural gas to generate energy, making it a more cost-effective solution rather than to add additional storage technology. However, this may only apply to an islanded operation, where larger capacity of storage is needed to replace the higher cost of energy generated from fossil fuels, or to attain constant production of 100% renewable energy. In this case, energy storage system is used to minimize power deviation between the actual fluctuating output power of renewable generation and the desired power into the grid. Consequently the sizing result of hybrid energy storage strongly depends on this function, which is why less capacity can be implemented to compensate the difference. Therefore, the total cost of installing a hybrid energy storage with the desired capacity and confidence level can match up with the total penalty cost if the power producer decided not to install any energy storage.
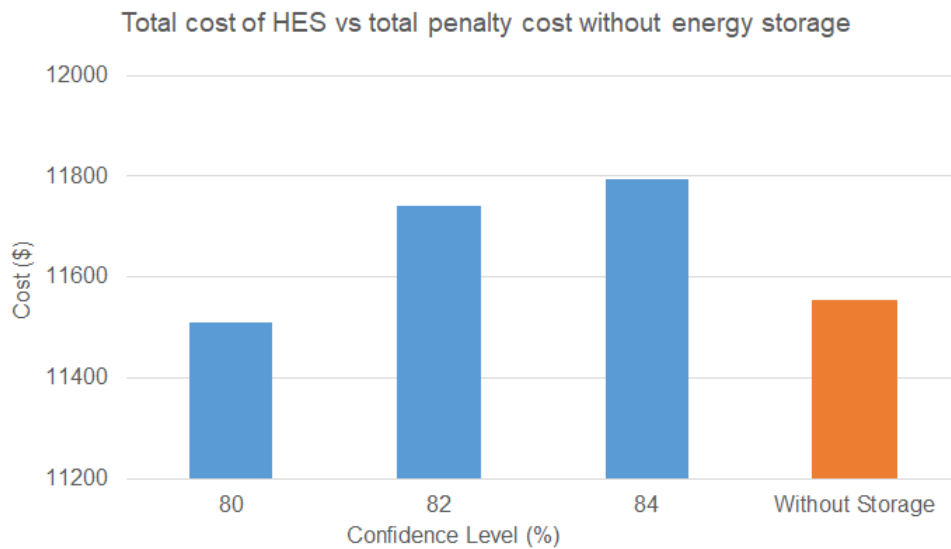
Figure 5.30: Comparison of hybrid energy storage's total cost and penalty cost without adding energy storage system

## 5.4. Conclusion

After three-level of decomposition processing, the true components and the noise in the balancing power is fully separated. The last approximations signal which contains low-frequency signal is extracted and fed to/drawn from the battery, while supercapacitor handle all the high-frequency components. Peak power before and after the wavelet transformation reduces from 0.65 kW to finally 0.21 kW, relieving the burdens on the battery system.

By combining the behavior of the energy storage components, the optimal total cost of hybrid energy storage technology considering uncertainty is accomplished by GA optimization using a CCP. Increase in the confidence level contributes to higher capacity of both devices, entailing higher total cost of the hybrid energy storage. However, higher capacity avoids over-charging/discharging which affects the energy storage's lifetime. The total cost of hybrid energy storage in each confidence level shows that the investment is suitable to replace the traditional battery energy storage system. A hybrid energy storage with up to 90% confidence level, or up to 3 kWh of battery and 0.3 kWh of supercapacitor capacity, is more economically feasible in handling the power fluctuation compared to a single battery energy storage device.

<div align="right">

# **6**

</div>

# Conclusions and Future Work

## **6.1.** Conclusions

The main aim for this work is to find the optimal hybrid energy storage (HES) sizing and the effective operation strategy for smoothing intermittent renewable energy power output. The evaluation is addressed by investigating the cost and the performance as well as the lifetime of the HES components. In this work, the main research questions are:

*What is the effective operation strategy of a hybrid energy storage for smoothing intermittent RESs power output?*

Storage devices have proved to reduce the uncertainty or power fluctuation of wind and PV generation in a power system. A HES which consists of battery and supercapacitor is chosen to smooth the renewable power output to obey the power grid's requirement. Both devices are complementary in terms of their ability to provide high-power characteristics as well as high-energy density to feed the balancing power, which is the deviation between the actual and the allowable power connected to the PCC.

The power sharing or distribution between the HES devices affects HES performance strongly. According to the characteristics of each battery and supercapacitor, frequency-based power-sharing is proposed as the operation strategy based on frequency. The wavelet transformation method is applied to firstly analyze the spectrum of balancing power. Secondly the method is able to divide the compensation frequency band for each battery and supercapacitor. While battery is assigned to provide the low frequency portion of the balancing power, supercapacitor on the other hand provides the high frequency portion. The results show that the supercapacitor peak fluctuations of battery power are moderated with the inclusion of supercapacitor in the system, providing lower peaks and slower derivative of power drawn from/fed to the battery.

The result from the power sharing is suitable in terms of extending the battery's lifetime. Battery lasts for 1.3 years in a conventional energy storage system, while it can last up to 6 years with the help of supercapacitor. Therefore, in terms of the life loss and replacement number, battery in a HES which implement wavelet-based power sharing can perform better compared compared to the conventional/single energy storage system.

*How to formulate the optimal hybrid energy storage sizing along with the power management system of the system considering uncertainty?*

In this paper, the characteristics of wind power and PV power random output were considered in the HES capacity sizing method. A chance-constrained programming handles the uncertainty of

wind and PV power output, and a solving method using a Monte Carlo simulation is incorporated with genetic algorithm optimization. The develped model could accommodate uncertain factors and handle fluctuation constraint in the power grid in a flexible way. In the premise of ensuring that the probability of smoothing the fluctuation power exceeding less than a certain confidence level $\alpha$, power and energy capacity of both battery and supercapacitor are obtained.

From the results it is clear that the energy capacity of hybrid energy storage is closely related to the value of confidence level $\alpha$. The value of α closer to 100%, the bigger penetration capacity, the more power fluctuation are satisfied. The lower confidence level ($\alpha$), the less battery and supercapacitor capacity to satisfy all power fluctuations. By not adequately sized, violation of the state of charge limits of the energy storage occurred and experience more frequent charging and discharging. Lower confidence level results in shorter lifetime and early failure. The degradation of the battery is more prominent due to the frequent battery charging/discharging cycles. Therefore, according to the network reliability and power fluctuation requirements, a reasonable choice of confidence level α is necessary.

Cost-risk curves illustrate the balance between the HES cost and the power fluctuation smoothing capability of the HES. Hybrid energy storage proved to be a viable technology when compared to the conventional/single energy storage device system. An optimal energy storage sizing interval is decided considering the investment cost, the risk of renewable power curtailment, and the total life cycle cost over the project's lifetime. The results show that, with the confidence level of smoothing requirement up to 90%, system contains two energy storage has a lower total cost than a single-sourced energy storage system.

## 6.2. Future Work

There is still further in-depth analysis to be made to get a more accurate HES design, by incorporating multi-objective design methods considering the following factors.

1. HES sizing

   HES capacity sizing method can take into account more uncertain factors such as reducing generation pollution, load growth, greenhouse gases, fuel consumption, and costs. Determining the capacity of HES considering the mentioned objective function is proposed for future researches.

2. HES power converter topology

   HES design for system stabilization and power quality improvement is not fully addressed. Various topologies can be used in the future for HES connection to microgrid, also by taking into account the converter cost and efficiency.

3. HES power sharing method
   The proposed approach uses a wavelet-based power sharing method without any prediction technique. However, it can be easily implemented in real-time applications with hardware implementation. To move beyond the simulation level, tehcnical/practical issues such as data acquisition, communication media and protocol, data management, and selection of processor, and other requirements still need to be considered.

# Bibliography

[1] PowerWeb, *Wind Energy and Solar | Installed GW Capacity - Global and by Country,* .

[2] S. Hajiaghasi, A. Salemnia, and M. Hamzeh, *Hybrid energy storage system for microgrids applications: A review,* Journal of Energy Storage **21**, 543 (2019).

[3] T. Bocklisch, *Hybrid energy storage systems for renewable energy applications,* Energy Procedia **73**, 103 (2015).

[4] E. M. Krieger, *Effects of variability and rate on battery charge storage and lifespan,* , 138 (2013).

[5] O. Erdinc, B. Vural, and M. Uzunoglu, *A wavelet-fuzzy logic based energy management strategy for a fuel cell/battery/ultra-capacitor hybrid vehicular power system,* Journal of Power Sources **194**, 369 (2009).

[6] P. Li, R. Dargaville, Y. Cao, D. Y. Li, and J. Xia, *Storage Aided System Property Enhancing and Hybrid Robust Smoothing for Large-Scale PV Systems,* IEEE Transactions on Smart Grid **8**, 2871 (2017).

[7] F. Birol, *Market analysis and forecast from 2018 to 2023,* (2018).

[8] E. Lannoye, *Renewable energy integration: practical management of variability, uncertainty, and flexibility in power grids [book reviews],* IEEE Power and Energy Magazine **13**, 106 (2015).

[9] American Physical Society, *Integrating Renewable Electricity on the Grid*, Tech. Rep. (2011).

[10] H. Ibrahim, A. Ilinca, and J. Perron, *Energy storage systems—characteristics and comparisons,* Renewable and sustainable energy reviews **12**, 1221 (2008).

[11] E. Chemali, M. Preindl, P. Malysz, and A. Emadi, *Electrochemical and electrostatic energy storage and management systems for electric drive vehicles: State-of-the-art review and future trends,* IEEE Journal of Emerging and Selected Topics in Power Electronics **4**, 1117 (2016).

[12] H. Bitaraf, S. Rahman, and M. Pipattanasomporn, *Sizing Energy Storage to Mitigate Wind Power Forecast Error Impacts by Signal Processing Techniques,* IEEE Transactions on Sustainable Energy **6**, 1457 (2015).

[13] B. Wang, B. Zhang, and Z. Hao, *Control of composite energy storage system in wind and PV hybrid microgrid,* IEEE Region 10 Annual International Conference, Proceedings/TENCON **55**, 1677 (2013).

[14] Lina Li and Li Yang, *A chance-constrained programming based energy storage system sizing model considering uncertainty of wind power,* , 51 (2013).

[15] F. Zhang, K. Meng, Z. Xu, Z. Dong, L. Zhang, C. Wan, and J. Liang, *Battery ESS Planning for Wind Smoothing via Variable-Interval Reference Modulation and Self-Adaptive SOC Control Strategy,* IEEE Transactions on Sustainable Energy **8**, 695 (2017).

[16] Q. Jiang, Y. Gong, and H. Wang, *A battery energy storage system dual-layer control strategy for mitigating wind farm fluctuations,* IEEE Transactions on Power Systems **28**, 3263 (2013).

[17] W. Ma, W. Wang, X. Wu, R. Hu, F. Tang, and W. Zhang, *Control strategy of a hybrid energy storage system to smooth photovoltaic power fluctuations considering photovoltaic output power curtailment,* Sustainability (Switzerland) **11** (2019), 10.3390/su11051324.

[18] X. Yang, H. Yue, and J. Ren, *Fuzzy Empirical Mode Decomposition for Smoothing Wind Power with Battery Energy Storage System,* IFAC-PapersOnLine **50**, 8769 (2017).

[19] M. T. Li, S. S. Choi, K. J. Tseng, Y. Yuan, and C. C. Sun, *Design of energy storage scheme for the smoothing and dispatch planning of large-scale wind power generation,* Proceedings of the 5th IEEE International Conference on Electric Utility Deregulation, Restructuring and Power Technologies, DRPT 2015 , 2113 (2016).

[20] E. Thorbergsson, V. Knap, M. Swierczynski, D. Stroe, and R. Teodorescu, *Primary Frequency Regulation with Li-Ion Battery Based Energy Storage System - Evaluation and Comparison of Different Control Strategies,* Telecommunications Energy Conference 'Smart Power and Efficiency' (INTELEC), Proceedings of 2013 35th International , 1 (2013).

[21] J. Wang, *Battery Impact Study on Stressed Distribution Grid,* (2016).

[22] N. Narayan, T. Papakosta, V. Vega-Garita, Z. Qin, J. Popovic-Gerber, P. Bauer, and M. Zeman, *Estimating battery lifetimes in Solar Home System design using a practical modelling methodology,* Applied Energy **228**, 1629 (2018).

[23] R. Zhang, B. Xia, B. Li, L. Cao, Y. Lai, W. Zheng, H. Wang, and W. Wang, *State of the art of lithium-ion battery soc estimation for electrical vehicles,* Energies **11**, 1820 (2018).

[24] B. Xu, Y. Shi, D. S. Kirschen, and B. Zhang, *Optimal regulation response of batteries under cycle aging mechanisms,* 2017 IEEE 56th Annual Conference on Decision and Control, CDC 2017 **2018-January**, 751 (2018).

[25] *Development of energy storage technology,* in *Grid-scale Energy Storage Systems and Applications,* edited by F.-B. Wu, B. Yang, and J.-l. Ye (Elsevier, 2019) pp. 1–15.

[26] L. Lin, R. Yang, and D. Yu, *Design of Hybrid Energy Storage for Photovoltaic Power Fluctuation Smoothing Based on Frequency Analysis,* , 954 (2016).

[27] P. L. Mao and R. K. Aggarwal, *A novel approach to the classification of the transient phenomena in power transformers using combined wavelet transform and neural network,* IEEE Transactions on Power Delivery **16**, 654 (2001).

[28] S. M. Ahmeda and M. Abo-Zahhad, *A new hybrid algorithm for ECG signal compression based on the wavelet transformation of the linearly predicted error,* Medical Engineering & Physics **23**, 117 (2001).

[29] J. Peng, R. Wang, H. Liao, Y. Zhou, H. Li, Y. Wu, and Z. Huang, *A real-time layer-adaptive wavelet transform energy distribution strategy in a hybrid energy storage system of evs,* Energies **12**, 440 (2019).

[30] V. Nourani, M. Komasi, and A. Mano, *A multivariate ANN-wavelet approach for rainfall-runoff modeling,* Water Resources Management **23**, 2877 (2009).

[31] B. Zakeri and S. Syri, *Electrical energy storage systems: A comparative life cycle cost analysis,* Renewable and Sustainable Energy Reviews **42**, 569 (2015).

[32] A. Roy and M. A. Kabir, *Relative life cycle economic analysis of stand-alone solar pv and fossil fuel powered systems in bangladesh with regard to load demand and market controlling factors,* Renewable and Sustainable Energy Reviews **16**, 4629 (2012).

[33] N. Yang and F. Wen, *A chance constrained programming approach to transmission system expansion planning,* Electric Power Systems Research **75**, 171 (2005).

[34] T. Summers, J. Warrington, M. Morari, and J. Lygeros, *Stochastic optimal power flow based on convex approximations of chance constraints,* in *2014 Power Systems Computation Conference* (IEEE, 2014) pp. 1–7.

[35] D. H. Loughlin and S. R. Ranjithan, *Chance-constrained genetic algorithms,* in *Proceedings of the 1st Annual Conference on Genetic and Evolutionary Computation-Volume 1* (Morgan Kaufmann Publishers Inc., 1999) pp. 369–376.

[36] B. Haihong, W. Xufang, D. Maosheng, and Z. Hong, *Optimal hybrid capacity configuration for distributed energy storage systems.* International Journal of Simulation–Systems, Science & Technology **17** (2016).

[37] P. Zhao, Y. Dai, and J. Wang, *Design and thermodynamic analysis of a hybrid energy storage system based on a-caes (adiabatic compressed air energy storage) and fess (flywheel energy storage system) for wind power application,* Energy **70**, 674 (2014).

[38] S. Wen, H. Lan, Y.-Y. Hong, C. Y. David, L. Zhang, and P. Cheng, *Allocation of ess by interval optimization method considering impact of ship swinging on hybrid pv/diesel ship power system,* Applied energy **175**, 158 (2016).

[39] H. Jia, Y. Mu, and Y. Qi, *A statistical model to determine the capacity of battery–supercapacitor hybrid energy storage system in autonomous microgrid,* International Journal of Electrical Power & Energy Systems **54**, 516 (2014).

[40] M. Masih-Tehrani, M.-R. Ha'iri-Yazdi, V. Esfahanian, and A. Safaei, *Optimum sizing and optimum energy management of a hybrid energy storage system for lithium battery life improvement,* Journal of Power Sources **244**, 2 (2013).

[41] Y. Zhang, Z. Jiang, and X. Yu, *Control strategies for battery/supercapacitor hybrid energy storage systems,* in *2008 IEEE Energy 2030 Conference* (IEEE, 2008) pp. 1–6.

[42] D. B. W. Abeywardana, B. Hredzak, and V. G. Agelidis, *Single-phase grid-connected lifepo battery–supercapacitor hybrid energy storage system with interleaved boost inverter,* IEEE Transactions on Power Electronics **30**, 5591 (2014).

[43] S. Bae, S. U. Jeon, and J.-W. Park, *A study on optimal sizing and control for hybrid energy storage system with smes and battery,* IFAC-PapersOnLine **48**, 507 (2015).

[44] A. Maleki and F. Pourfayaz, *Sizing of stand-alone photovoltaic/wind/diesel system with battery and fuel cell storage devices by harmony search algorithm,* Journal of Energy Storage **2**, 30 (2015).